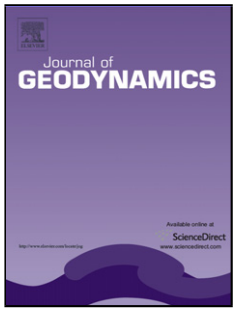

Title: Late Cenozoic contractional evolution of the current arc-volcanic region along the southern Central Andes (35°20′S)

Author: Felipe Tapia Marcelo Farías Maximiliano Naipauer Jacqueline Puratich

PII: S0264-3707(15)00002-2
DOI: http://dx.doi.org/doi:10.1016/j.jog.2015.01.001
Reference: GEOD 1347

To appear in: *Journal of Geodynamics*

Received date: 20-6-2014
Revised date: 22-12-2014
Accepted date: 6-1-2015

Please cite this article as: Tapia, F., Farías, M., Naipauer, M., Puratich, J.,Late Cenozoic contractional evolution of the current arc-volcanic region along the southern Central Andes (35^{circ}20'S), *Journal of Geodynamics* (2015), http://dx.doi.org/10.1016/j.jog.2015.01.001

Late Cenozoic contractional evolution of the current arc-volcanic region along the southern Central Andes (35º20'S)

Felipe Tapia[1], *Marcelo Farías*[1], *Maximiliano Naipauer*[2] *and Jacqueline Puratich*[1]

[1]*Departamento de Geología, Universidad de Chile, Santiago, Chile.*

[2]*Instituto de Estudios Andinos "Don Pablo Groeber", Departamento de Ciencias Geologicas, FCEN, Universidad de Buenos Aires-CONICET, Buenos Aires, Argentina*

Abstract

The Andean internal zone records deformation, uplift and erosion that serve as proxies of variations on mountain building dynamics. Hence, the study of this region would give keys to understand the factors controlling the orogenic evolution. Structural, stratigraphic and geochronological data in the Andean internal zone at 35°20'S evidence that this region has only underwent contractional deformation since the late Miocene up to present, differing from coeval Pleistocene extensional tectonics affecting the retro-arc. Contractional deformation was characterized by the development of a piggy-back basin in the latest Miocene filled by synorogenic deposits. Afterward, an out-of-sequence thrusting event affected the region since at least the Pliocene until the Present. Shortening in the inner part of the Andean orogen would be favored by both the high orthogonality of the out-sequence structures with respect to the plate convergence vector and by the minor resistance to shortening produced by the southward decrease of the orogen height and by the removal of material via erosion of the uplifted mountain belt. In contrast, oblique structures, as those described farther north, accommodate strike-slip displacement. Likewise, we propose that

erosion from the inner orogen favored the prolongation of the out-of-sequence thrusting event until the Present, differing from the situation north of the 34°S where this event ended by the Pliocene.

Keywords

Out-of-sequence thrusting, synorogenic deposits, Andean Cenozoic evolution.

1 Introduction

The current volcanic arc region along the southern Central Andes corresponds to the internal part of an orogen formed in an oceanic-continent subduction regime, developed near the present-day Pacific-Atlantic drainage divide (Fig. 1a). Subduction of the oceanic Nazca plate beneath the South American plate has resulted in almost continuous magmatism during the system's evolution, in addition to the involved stress transfer to the overriding plate. This process has led to crustal shortening and thickening and the consequent uplift in the overriding South American plate mainly during the late Cenozoic (Charrier et al., 2007, 2014; Farías et al., 2008, 2010; Folguera et al., 2011; Giambiagi and Ramos, 2002; Giambiagi et al., 2003, 2008; Ramos et al., 2014; Ramos and Folguera, 2005; Ramos and Kay, 2006).

Fig. 1 here

Despite the along-strike continuity of the mountain belt in the southern Central Andes, the orogenic volume and maximal crustal thickness gradually decreases to the south without exhibiting relevant changes in the decrease gradient (*e.g.*, Pose et al., 2005; Tassara et al., 2005; Tassara and Echaurren, 2012). However, it has been proposed that the internal zone

of the orogen evolved differently north and south of 35°S since the late Miocene (see Charrier et al., 2014 and references therein). In fact, the contractional stage north of 35ºS ended by the Pliocene (Giambiagi et al., 2003), which was followed by strike-slip deformation until today (Farías et al., 2010), whereas south of 35°S, shortening would have been interrupted by an extensional episode in the early Pleistocene, which affected the retro-arc region and spread to the arc region (Folguera et al., 2006b, 2008, 2011, 2012; Ramos and Folguera, 2011; Spagnuolo et al., 2012). This event was preceded by a late Miocene eastward magmatic expansion and shortening migration to the foreland that produced the uplift of the San Rafael Block (see Ramos and Kay, 2006, and reference therein).

The extensional episode was characterized by the early Pleistocene-Holocene development of several NW-trending depressions with a concomitant development of intraplate volcanism in the retro-arc region between 35° and 40°S (*cf.* Ramos et al., 2014 and reference therein). This evolution is supported by several structural (Folguera et al., 2004, 2006b, 2008, 2010; Garcia Morabito and Folguera, 2005; Ramos and Kay, 2006; Rojas-Vera et al., 2010, 2014), geophysical (Folguera et al., 2007a, 2012), and petrological studies (Folguera et al., 2009; Kay et al., 2006; Ramos and Folguera, 2011). According to Folguera et al. (2006b; 2008), the northernmost depression extended up to the arc region slightly south of 35ºS. There, they infer that the high volume of silicic volcanic material extruded by the Calabozos caldera since the early Pleistocene (*cf.*, Hildreth et al., 1984) was controlled by extensional tectonics related to the development of the Las Loicas Trough, the northernmost extensional depression in Argentina. Nevertheless, there is no reported evidence for extension in this area, exposing the lack of appropriate structural studies and

the poor knowledge of the Quaternary evolution of the internal zone of the Andean orogen at the latitudes of this study.

The proposed extensional evolution for the current arc region south of 35°S contrasts with those reported to the north and farther south at 36°30´S. In both regions, contractional deformation has dominated the internal part of the Andean range since the late Miocene as an out-of-sequence thrusting event, even though it evolved to transcurrent deformation by the Pliocene in the north (Folguera and Ramos, 2009, Folguera et al., 2004, 2006a, 2007b; Giambiagi and Ramos, 2002; Giambiagi et al., 2003; 2014; Godoy et al., 1999; Rojas-Vera et al., 2014).

The eastward migration of shortening and expansion of the volcanic arc at these latitudes during the late Miocene has been interpreted as a consequence of a shallowing of the subducting slab, whereas the subsequent extension and intraplate volcanism has been explained by the steepening of the slab (see Ramos and Kay, 2006 and reference therein).

Nevertheless, extensional deformation has not been directly reported along the arc-region, but contractional deformation has been proposed for this area at a similar time (e.g., Farías et al., 2009). This is evidencing a decoupling between the deformation of the retro-arc and arc region during the event of slab shallowing and deepening, thus highlighting some concerns about the actual extent of the effects produced by the slab dynamics in the Andean evolution at these latitudes. In this context, this contribution addresses the question about the kinematic evolution of the arc-region in the scope of the actual extent of the extensional development reported in the retro-arc with respect to the contractional evolution that has characterized the late Cenozoic growth of the Andes.

In this context, this study focuses on determining the deformation that controls the Neogene to Quaternary evolution of the axial region of the Andes at 35°20'S. Our contribution mainly consists of new detailed field mapping and stratigraphic, structural, U/Pb age and apatite (U-Th)/He data. We focused particularly on a sedimentary unit corresponding to Neogene synorogenic deposits that record not only the erosional processes of the mountain belt but also constrain the timing of deformational events that affected this area and the source region related to the uplifted areas that supplied sediment to this basin. Our results show that the inner region of the mountain belt has been subjected to a continuous contractional regime from the middle Miocene to the Present, rather than the extensional setting inferred by previous studies. Furthermore, we discuss the deformation kinematics of the internal region of the Andean orogen and its differences with respect to the retro-arc region.

2 Tectonic setting of the southern Central Andes

The central Chile and Argentina region lies within the southern Central Andes, which are limited to north at *ca.* 33ºS by the Pampean flat-slab segment (Fig. 1a). The Andean margin at these latitudes is characterized by the subduction of the oceanic Nazca plate beneath the South American continent (Fig. 1a) with a slab dip of ~30°E, corresponding to the typical example of the "Chilean-type subduction" in the sense of Uyeda and Kanamori (1979).

The southern Central Andes at the latitude of this work are segmented into four trench-parallel continental morphostructural units (Fig. 1b). From west to east, these are as follows: (1) the Coastal Cordillera, composed of Paleozoic metamorphic/crystalline basement and Jurassic-Cretaceous intrusive and volcanic rocks (Charrier et al., 2007); (2)

110 the Central Depression, with a Quaternary volcano-sedimentary cover and a Mesozoic and
111 Cenozoic basement (Farías et al., 2008); (3) the Principal Cordillera, consisting of
112 Mesozoic and Cenozoic rocks (Charrier et al., 2007, Ramos, 2000a); and (4) the Foreland,
113 composed of Neogene to Quaternary deposits that originated mainly by the erosion of the
114 eastern Principal Cordillera and covering Mesozoic rift-related sedimentary rocks (Charrier
115 et al., 2014). To the east, the Foreland is broken by the uplifted Paleozoic-Triassic
116 metamorphic/crystalline basement of the San Rafael Block (Fig. 1b) (González Díaz, 1972;
117 Ramos et al., 2014 and references therein).

118 In this study, we subdivide the Principal Cordillera into a western and an eastern Principal
119 Cordillera according to their geological and structural features. The western Principal
120 Cordillera consists mostly of Cenozoic sequences (Fig. 1b) (Charrier et al., 2007). In
121 contrast, the eastern Principal Cordillera is characterized by the exposure of Mesozoic
122 sedimentary rocks covered by Cenozoic volcanic and sedimentary synorogenic deposits
123 (Fig. 1b) (Ramos, 2000a and references therein). The boundary between the western and
124 eastern Principal Cordillera is close to the axis of the Principal Cordillera and coincides
125 with the current active volcanic arc and the Pacific-Atlantic watershed. This is the location
126 of the study region (Fig. 1b).

127 The evolution of the southern Central Andes between 35º and 36ºS comprises successive
128 episodes of contractional, extensional and transcurrent deformation (*e.g.*, Charrier et al.,
129 2007, 2014; Ramos, 2000b). The last extensional event occurred between the Eocene and
130 the late Oligocene along the western Principal Cordillera (Fig. 1b), forming the north-
131 trending intra-arc extensional Abanico basin (Charrier et al., 1996, 2002; Godoy et al.,
132 1999). This basin was filled with up to approximately 2,500 m of volcanic and

133 volcanoclastic rocks with some fluvial and lacustrine deposits (Charrier et al., 2002). The
134 basin-related deposits have been grouped into the Abanico Formation near Santiago and
135 south of 35°S, the Coya-Machalí Formation between 34° and 35°S, and the Cura-Mallín
136 Formation south of 36ºS. Hereafter, these deposits will be referred as the Abanico
137 Formation and the related basin as Abanico Basin. During the early Miocene, the basin
138 began to be inverted in a process that concentrated most of shortening at its edges (Fock et
139 al., 2006; Farías et al., 2010).

140 Following the initial stages of basin inversion, after ~18 Ma, deformation migrated
141 eastwards, affecting the Mesozoic deposits that had accumulated in the Neuquén Basin
142 (Fig. 1a), a back-arc basin formed during a widespread extensional tectonic event in South
143 America (Charrier, 1979; Charrier et al., 2007; Mpodozis and Ramos, 1989; Uliana et al.,
144 1989). The eastward migration of the deformation was characterized by the development of
145 the hybrid thick- and thin-skinned Malargüe fold-and-thrust belt (Malargüe FTB)
146 (Kozlowsky et al., 1993; Manceda and Figueroa, 1995) and subsequently by the uplift of
147 the San Rafael Block (González Díaz, 1972). Simultaneously, the related-arc magmatism
148 also expanded and migrated to the east up to 600 km from the current Pacific trench,
149 reaching the San Rafael Block during the late Pliocene (Charrier et al., 2007; Kay et al.,
150 2005; Litvak and Folguera, 2008; Ramos et al., 2014). During this Neogene contractional
151 evolution, synorogenic deposits accumulated in the Río Grande foreland basin starting at
152 *ca.* 18 Ma (Fig. 1b), which was cannibalized due to the progressive eastward migration of
153 shortening (Silvestro and Atencio, 2009). The expansion of the magmatic arc and the
154 eastward migration of the deformation front have been explained by crustal erosion caused

155 by subduction (Kay et al., 2005) along with a shallowing of the subducted slab during the
156 late Cenozoic (Ramos and Kay, 2006; Ramos et al., 2014; Spagnuolo et al., 2012).

157 In the Quaternary, the retro-arc region experienced an extensional event evidenced by
158 normal faulting of the late Miocene uplifted peneplain that developed over the San Rafael
159 Block (Folguera et al., 2008, 2007a, 2007b). This period was accompanied by basaltic
160 volcanism (Ramos and Folguera, 2011) and the development of huge calderas of rhyolitic
161 to dacitic composition and subordinate basalts that were emplaced near the axis of the
162 Cordillera during the last one million years (Grunder and Mahood, 1988; Grunder, 1987;
163 Hildreth et al., 1984). The flood basalts of the retro-arc region have been interpreted as
164 direct melts of the asthenosphere associated with the steepening of the subducted slab
165 during the Quaternary (Kay et al., 2006). Likewise, the origin of rhyodacitic volcanic
166 deposits near the axis of the Cordillera has been proposed to be the result of crustal
167 delamination produced by the injection of asthenosphere during the steepening of the
168 subducted slab (Ramos et al., 2014).

169 ## 3 Geology of the study region

170 ### 3.1 Generalities

171 The study region involves the eastern limit of the Abanico Formation and the westernmost
172 outcrops of the Mesozoic series of the eastern Principal Cordillera (Fig. 1b). This zone
173 coincides with a structural transition between the deformation that characterizes the domain
174 of the Abanico Basin to the west and the Malargüe FTB to the east (Fig. 1b). Furthermore,
175 the landscape of this zone is marked by the presence of Quaternary arc-related volcanic

176 rocks forming a large plateau and edifices shaped by fluvial and glacial erosion and that
177 discordantly overlie older geological units and structures.

178 To characterize the geology of this area, we performed geological mapping of outcropping
179 rocks and structures, complemented with previously published and unpublished geological
180 maps (Gonzalez and Vergara, 1962; Grunder, 1987; Grunder and Mahood, 1988; Grunder
181 et al., 1987; Hildreth et al., 1984; Naranjo et al., 1999). This allowed the construction of a
182 schematic cross section constrained by new chronological data (Fig. 6).

183 In relation to previous works, the regional map made by González and Vergara (1962) is
184 the sole study of this type performed in the study region, even though certain local
185 geothermal and volcanic studies have also been conducted in this region (Grunder, 1987;
186 Hildreth et al., 1984; Naranjo et al., 1999; Naranjo and Haller, 2002). González and
187 Vergara (1962) characterized the structure and described the stratigraphic units of the
188 region at a 1:250,000 scale. When describing the Mesozoic series, the authors defined and
189 named them with local names that differed from those used in the Argentinean and Chilean
190 stratigraphic nomenclature. To avoid misunderstandings, we use the Argentinean
191 nomenclature to compare and correlate the geology of both countries in this work.

192 **3.2 Geological Units**

193 The geology of the study region is displayed in the geologic map of Fig. 2a. The major
194 stratigraphic units present in this area can be divided into four main associations: (1) the
195 Mesozoic sediments of the Neuquén basin, which are subdivided into three main units, the
196 Cuyo, Lotena and Mendoza groups; (2) the Abanico Formation; (3) the synorogenic
197 deposits, here grouped into the Colorado Strata Unit; and (4) the Plio-Quaternary volcanic

198 deposits. In addition, the zone features two main intrusive bodies of granodioritic to
199 granitic composition of late Miocene age. The nomenclature, lithology, age and tectonic
200 setting of all these units are briefly described below, except for the synorogenic deposits,
201 which are described later in Section 3.3.

202 Fig. 2 here

203 The eastern area of the study region is mostly dominated by Mesozoic sedimentary series
204 (Fig. 2a), which are associated with cycles of marine transgression and regression that
205 occurred before the uplift of the Andean Cordillera. The oldest outcropping unit
206 corresponds to the Cuyo Group (Sinemurian-Bajocian), which consists of off-shore shelf
207 black shales grouped into the Tres Esquinas Formation and sandy fluvio-estuarine facies of
208 the prograding Lajas Formation (Gulisano and Gutiérrez Pleimling, 1995). These two
209 formations are separated by an erosional unconformity. The Cuyo Group is overlain by
210 deltaic to shallow-marine clastic deposits belonging to the Lotena and the La Manga
211 formations of Bajocian and Callovian ages, respectively. The gypsum layers of the
212 Auquilco Formation (Oxfordian) overlie both formations. These formations make up the
213 Lotena Group. The youngest Mesozoic unit is the Mendoza Group, composed of the red
214 continental sandstones of the Tordillo Formation, the organic-rich deep-marine shaly marls
215 of the Vaca Muerta Formation, and the shallow-marine limestones of the Chachao
216 Formation.

217 In the western part of the study region, the Abanico Formation crops out (Fig. 2a) and is
218 composed of a series of basic to intermediate volcanic-volcanoclastic rocks with
219 intercalations of limestones, siltstones and very coarse- to fine-grained sandstones, as well

as conglomerates with a significant volcanic component. Based on mammal fossil fauna and radiometric dating, the age of this formation north of the study region has been determined to be between the Eocene and the late Oligocene (Charrier et al., 2007, 2002, 1996; Godoy et al., 1999). This unit is discordantly covered by the volcanic Cola de Zorro Formation and a clastic synorogenic unit referred to here as the Colorado Strata Unit because of its excellent exposure along the homonymous valley.

The previous units are unconformably overlain by Plio-Quaternary arc-related volcanic rocks. We separated these volcanic rocks into three groups according to their age. In the western area, the Abanico Formation and the synorogenic deposits are covered by the almost undeformed basaltic-andesitic lava series of the Cola de Zorro Formation, which forms a large volcanic plateau emplaced over a low-relief surface now dissected by fluvial and glacial valleys. These rocks are distributed along the Colorado river valley and reach a maximum preserved thickness of 150 m. At 35.7ºS, Drake (1976) reported an age span for this formation between 2.47 and 0.96 Ma. In the study region, an age obtained using the K-Ar method (whole-rock) is 2.02 ± 0.10 Ma near the base of the sequence (Fig. 2a) (Hildreth et al., 1984).

The second group of volcanic rocks corresponds to the deposits associated with the Peteroa-Azufre Volcano unit (Naranjo et al., 1999). This is the oldest unit of the Planchón Peteroa Volcanic Complex and consists of a series of basalts, basaltic-andesites, andesites and dacites cropping out along the northern slope of the Colorado river valley and farther north of the study area (Naranjo et al., 1999). The oldest and youngest reported K-Ar ages for this complex are 1.20±0.03 Ma (Naranjo et al., 1999) and 0.55±0.05 Ma (Hildreth et al.,

1984), respectively, even though this complex records a series of historical eruptive events (Naranjo et al., 1999).

The third volcanic group corresponds to the Loma Seca Formation (Grunder et al., 1987; Hildreth et al., 1984), which is distributed across almost the entire study region (Fig. 2a). The deposits are emplaced in deep paleovalleys excavated in the Mesozoic series and synorogenic deposits and form several volcanic plateaux due to the high volume of erupted material. The formation consists of dacitic to rhyo-dacitic volcanic deposits derived from the eruption of 150 to 300 km^3 of magma from the Calabozos caldera (Hildreth et al., 1984), which lies in the southeast sector of the study region (Fig. 2). The age of the Loma Seca Formation is constrained by K-Ar dating, yielding ages between 0.79±0.15 and 0.14±0.04 Ma (Hildreth et al., 1984), even though certain deposits were clearly emplaced after the last glacial event 4,400 years before the present (Espizua, 2005; Naranjo and Haller, 2002).

Two intrusive units that intruded Mesozoic and Cenozoic deformed rocks crop out in the area. In the eastern sector, the late Miocene Potrerillos pluton intrudes a Mesozoic series (Fig. 2a) and yields a zircon U/Pb age of 11.3 ± 0.20 Ma (error level at 2σ for all the ages reported in this study) obtained in this work (Fig. 2b; see Appendix A for the complete data set and analytical details). Given its petrological features and location, this pluton correlates with an intrusive body cropping out in the northeastern edge of the study region, near the international border (Fig. 2a). In the western sector, the Río Negro pluton intrudes the Abanico Formation (Fig. 2a) and yields a zircon U/Pb age of 10±0.05 Ma, also determined in this study (zircon U-Pb age, Fig. 2c). Outside the study region, approximately 13 km west of the Río Negro pluton along the Colorado river valley, the La Gallina granodioritic

pluton also intrudes the Abanico Formation, (Fig. 1c) and was also dated by this study, yielding a zircon U-Pb age of 8.688 ± 0.071 Ma (Fig. 2d). These plutons belong to the late Miocene intrusive belt (*e.g.*, Farías et al., 2008; 2010) and evidence the magmatic activity in the western Principal Cordillera during the late Miocene.

3.3 The Colorado Strata Unit

The sedimentary strata grouped in the Colorado Strata Unit were deposited unconformably over the Mesozoic series (Fig. 3a). This unit crops out mostly in the central part of the study region (Fig. 2a). These sediments are unconformably overlain by Plio-Quaternary volcanic rocks (Fig. 3c), and the unit is limited to the west by the El Novillo thrust and to the east by the Valle Grande and Debia anticlines (Fig. 2a).

Fig. 3 here

The Colorado Strata Unit reaches up to 400 m in thickness. The conglomerates and sandstones that comprise this unit are moderate-to-poorly sorted, very coarse to medium grained and texturally and mineralogically immature. The conglomerate beds are 50 cm to 2 m thick and distributed in coalescent lenses, whereas sandstone beds are less than 1 m thick. The sandstones exhibit mostly planar stratification, even though they also show sedimentary structures such as cross stratification (Fig. 3d). The sandstones are also present as decametric lenses interbedded in the conglomerates, particularly between the conglomeratic coalescent lenses, and often exhibit lateral accretion (Fig. 3e).

Conglomerates are massively bedded, both clast and matrix supported, with some imbricated clasts levels, oligomictic, and with a predominance of volcanic and subordinate

granitoid rock clasts (Figs. 3f and g). Paleocurrent measurements obtained from the eastern outcrops indicate a transport direction from the east (Fig. 3b).

Fig. 4 here

The conglomerate clasts are 10-40 cm in size, subangular to subrounded, and poorly sorted. The matrix features angular to subangular and poorly sorted grains and is mainly composed of feldspars and lithic fragments. The sandstones are lithic to feldspathic arenites composed of poorly sorted, immature, and coarse- to medium-grained sands. The major constituents of the sandstones are lithic fragments and plagioclase feldspar (Fig. 4a). These lithic fragments are primarily volcanic fragments with porphyritic andesite and red sedimentary rock fragments (Figs. 4a, b, c, and e). The sedimentary fragments contain subrounded to rounded plagioclases and quartz in a red iron-oxide-rich matrix (Figs. 4a and b), very similar to the Tordillo Formation sandstones (Fig. 4d). The plagioclase feldspar components are coarse-grained, twined, and subhedral to euhedral altered crystals (Figs. 4a, c and e). The matrix of the sandstones corresponds to unidentifiable fragments altered to cryptocrystalline white mica and clay minerals (Figs. 4b and c).

The Colorado Strata Unit exhibits rotational onlaps, offlaps and apical wedges on the western flank of the Debia anticline (Fig. 2a and 3b). Because the sequence exhibits continuous cycles, without relevant vertical changes in bed thickness or facies, the change in dip is indicative of progressive unconformities in the growth strata. Based on the described features, this unit corresponds to synorogenic deposits.

According the described features of this unit, we interpret the depositional environment to have been an alluvial environment characterized by the successive deposition of debris

flows and sandy sheet flows, with the ephemeral development of braided rivers in a proximal zone and lateral sand accretion on the conglomeratic bars. These features can be interpreted as the development of proximal alluvial fans with successive cyclic changes in transport energy. Given the observations made on this sequence in relation to the structures present in the area (Fig. 3b), the changes in transport energy may be a result of slope changes due to the activity of contractional structures.

3.4 Structure

To track the late Cenozoic evolution of the region, two WNW-ESE cross sections compile the structural features in the northern and central areas of the study region (Fig. 5). These sections are constrained only by surface geology for the shallow levels because of the absence of seismic and well data in the area. We describe the structures according to their relative timing with respect to the Colorado Strata Unit given the synorogenic nature of this unit.

Fig. 5 here

3.4.1 Pre- and syn-depositional structures

The western sector of the study region along the Colorado river is dominated by the development of the Colorado anticline, a high-amplitude east-vergent anticline involving the Abanico Formation (Fig. 5a). This structure has a half-wavelength of 5 km and front- and backlimb dips of 40°-50°E and 20°W, respectively. The core of the Colorado anticline hosts the Río Negro pluton (Fig. 5a). Although there is no direct evidence to determine the timing of activity of this structure, we infer that the Colorado anticline was formed during the inversion of the Abanico Basin after 20 Ma, given the age of deformation farther north

330 (Charrier et al., 2002; Farías et al., 2010; Fock et al., 2006). This structure was likely active
331 at 10 Ma due to the emplacement of the Río Negro pluton at its core, and ceased activity
332 before the emplacement of the Cola de Zorro Formation at *ca.* 2.5 Ma.

333 Fig. 6 here

334 Two N-S-trending anticlines, the Valle Grande and the Debia anticlines, control the
335 contractional deformation in the eastern part of the region (Fig. 2a). The Valle Grande
336 anticline is an east-vergent and asymmetric fold plunging to the north and south. This
337 anticline involves the Cuyo and Lotena groups in its western limb and the Tordillo
338 Formation in its eastern limb. It runs along the Valle Grande river valley, with a gently
339 dipping backlimb (20°-30°W) and a very steeply dipping forelimb (50°-60°E), which is
340 indicative of its east vergence (Fig. 5a). In the Cerro Las Yeguas area, the Colorado Strata
341 Unit exhibits increasing thicknesses to the west (Figs. 6a and b), indicating that the
342 accumulation zone was to the west, likely near the eastern front of the Colorado anticline.
343 The angular unconformity between the synorogenic deposits and the back-limb of the Valle
344 Grande anticline (Figs. 6a and b) indicates that the anticline began to develop before the
345 synorogenic deposition. However, the lack of exposures of the base of the Colorado Strata
346 Unit prohibits inferences of their relationship at the beginning of deposition. The
347 accumulation of the synorogenic deposits continued after the development of the angular
348 unconformity observed in the Cerro Las Yeguas (Fig. 6a), as evidenced by progressive
349 unconformities related to the westward growth strata.

350 Along Debia creek, the most important structural feature is the Debia anticline. It is a broad
351 and symmetric structure plunging to the north, with a N-S strike and a 5 km-wide half-

352 wavelength (Fig. 2a). It deforms Mesozoic strata with the gypsum layer of the Auquilco
353 Formation in its core and the Tordillo, Vaca Muerta and Chachao Formations toward the
354 limbs. Growth strata in the Colorado Strata Unit developed on the western flank of this
355 anticline, indicating that deposition was simultaneous with the growth of the Debia
356 anticline.

357 **3.4.2 Post-depositional structures**

358 Three main thrusts that continued to be active after the deposition of the Colorado Strata
359 Unit characterize the study region. From west to east, they are named the El Novillo, Llolli
360 and Calabozos thrust systems.

361 The El Novillo thrust corresponds to a NE-SW-trending structure that limits the Colorado
362 Strata Unit to the east and the Abanico Formation to the west (Fig. 2a), putting the Abanico
363 Formation over the synorogenic deposits (Fig. 5a). In the hanging wall of the El Novillo
364 thrust, the Abanico Formation dips ~ 60°W, whereas the Colorado Strata Unit in the
365 footwall forms a tight syncline (Fig. 5a). In this area, the Colorado Strata Unit does not
366 exhibit either growth strata or progressive unconformities. Thus, the deformation linked to
367 this structure indicates that the El Novillo thrust was active after the deposition of the
368 synorogenic deposits and before the deposition of the Pleistocene Cola de Zorro Formation.

369 The Llolli thrust is located immediately to the east of the El Novillo thrust (Figs. 2a and
370 5a). This structure cuts the synorogenic deposits, repeating the Colorado strata in the
371 southern slope of the Colorado river (Fig. 6c). In the Cerro Las Yeguas locality, the Llolli
372 thrust only folds the synorogenic deposits (Figs. 6a and b). This structure ends below

373 undeformed Pleistocene volcanic rocks (Fig. 6c); thus, its activity is constrained between
374 the deposition of the Colorado Strata Unit and the Pleistocene.

375 Fig. 7 here

376 The third post-depositional structure is the Calabozos thrust system (Fig. 2a). This
377 structural system corresponds to east-vergent, low-angle reverse faults with three main
378 branches striking approximately N-S dipping *ca.* 30ºW (Fig. 5b and 7a), with a central
379 branch extending along 9 km long from the toe of the Cerro Las Yeguas in the Valle
380 Grande area to near the Potrerillos pluton to the south (Fig. 7a). The thrust is best exposed
381 in the Debia Creek. In this zone, the western branch ends to the south and a new branch
382 appears to the east extending to the south (Fig. 7a). Here, the system presents its maximal
383 surface separation of about 1.2 km. North and south of this area, the separation diminish to
384 300-500 m. The central branch at this creek develops a ~200 m width tectonic breccia that
385 includes rocks of the Loma Seca Formation (Fig. 7b and e). Between central and eastern
386 branches, the Colorado Strata Unit developed growth strata during deposition in a syncline
387 (Fig. 3b). North of the Debia Creek to Valle Grande, the thrust consists of two well-
388 developed branches offsetting the Loma Seca Formation, hillslope-related deposits, and
389 glacier-related deposits and landforms (Figs. 7b, c, d, e, f and h). Here, the thrust produces
390 a ~20 m scarp in both moraines and "*roches moutonnées*" (Fig. 7h), and has led to the
391 development of sag ponds and disturbances in the river network (Figs. 7c and d). To the
392 north, the offset decreases and disappears in the Valle Grande valley, where several relict
393 scarps and breccias are observed (Fig. 7f). Here, only western branch of the thrust can be
394 recognized. This branch can be observed up to the western slope of Valle Grande valley,
395 where a fault breccia aligned with the trace of the fault described to the south is evidence of

its northern extent. Considering the units deformed by the Calabozos thrusts system, it can be concluded that this fault has been active at least since the deposition of the Colorado Strata Unit.

4 Analytical constraints on the deformational and erosional evolution

4.1 U/Pb ages of the Colorado Strata Unit

Two samples located at the top of the Colorado Strata were collected (Fig. 8a) and dated via the zircon U-Pb method (LA-MC-ICP-MS). The analyzed samples correspond to a boulder-sized granite fragment from a conglomerate level (Fig. 8d) (sample TA11-22A) and the sandy levels surrounding the granitic boulder from the upper section of the Colorado Strata in Cerro Las Yeguas (Figs. 5a and b) (TA11-22B sample). The sample location appears in Fig. 2b, and the complete description of analytical methods and the results of the U-Pb geochronological determinations are provided in Appendix B.

Fig. 8 here

For the sandstone sample TA11-22B, 108 detrital zircons provide a pattern of detrital zircon U/Pb ages that constrain the maximum depositional age. The results show a spectra of concordant ages between *ca.* 6.8 Ma and *ca.* 305 Ma (Fig. 8c), bimodal maximum peaks at *ca.* 158 Ma (74%; ages between *ca.* 149.9 Ma and 166.6 Ma) and *ca.* 7 Ma (24%; ages between *ca.* 6.8 Ma and 7.9 Ma); and two single ages at *ca.* 305 Ma (Middle Pennsylvanian) and *ca.* 15 Ma (early Miocene). The maximum peak at *ca.* 7 Ma is the youngest and therefore corresponds the maximum depositional age of the upper section of the Colorado Strata (Fig. 8c).

For the sample TA11-22A, 30 analyzed zircon grains were used to determine the crystallization age of the granitic intrusive clast (Fig. 8b). The sample's results show a concordia age at 155.3 ± 3 Ma for 29 zircons (Fig. 8b) and a single age at 329.3 ± 6 Ma (Fig. 8b).

4.2 Apatite (U/Th/He) ages

Additionally, we obtained three apatite (U/Th)-He ages from rocks situated west of the Colorado Strata Unit to test the effects of exhumation of the western region during the evolution of the synorogenic unit as well as to better constrain its depositional age. Samples were taken along the Colorado river valley bottom from the Abanico Formation, the Río Negro pluton and the La Gallina pluton at approximately 1, 6 and 21 km west of the El Novillo thrust, respectively (Table 1, see Fig. 1c for location and Appendix C for details of the (U/Th)-He analytical methods and data).

Table 1 here

The results show that the plutons west of the El Novillo thrust were exhumed at *ca.* 3.8 Ma, whereas the Abanico Formation immediately west of this thrust were exhumed at *ca.* 1.5 Ma. The apatite (U/Th)-He ages obtained from the plutonic rocks indicate the cooling of plutonic rocks produced by exhumation because their crystallization ages are approximately 8 million years older. These exhumation ages are slightly older than the beginning of the deposition of the Cola de Zorro Formation, which was deposited unconformably over the Colorado Strata Unit and older units, sealing the activity related to the El Novillo thrust. Therefore, the thermochronologic ages of the plutonic rocks record the erosion in response to the uplift of the Colorado anticline and structures farther west. Because the deposition of

439 the Cola de Zorro Formation sealed the end of activity of the El Novillo thrust, the
440 youngest age in the Abanico Formation should be related to the valley development that
441 preceded the deposition of the Loma Seca Formation in paleovalleys starting at 0.9 Ma.

442 **5 Discussion**

443 **5.1 Sedimentary source of the synorogenic deposits**

444 The boulder-sized granite fragment dated to *ca.*155 Ma (sample TA11-22A) and the Upper
445 Jurassic zircon age population in the sandy sample (TA11-22B) suggest a derivation from
446 Upper Jurassic granites extensively exposed along the present-day Coastal Cordillera (Fig.
447 1b). However, the western flank of the Principal Cordillera, to the west of the study area,
448 uplifted during the early Miocene and reactivated during the late Miocene (Farías et al.,
449 2010, 2008). This would have prevented sedimentary input from the Coastal Cordillera,
450 even though the eastern domains of the Abanico Formation, particularly from the Colorado
451 anticline to the El Novillo thrust, could have corresponded to a clastic source of the
452 Colorado Strata Unit.

453 We propose that the main source for this age population is the Upper Jurassic Tordillo
454 Formation (Río Damas Formation in Chile), which is widely exposed throughout the study
455 region (see Fig. 1b). In fact, the petrographic descriptions of the sandstones and
456 conglomerates of the Colorado Strata Unit reveal red sedimentary clasts and lithics similar
457 to the petrography of the Tordillo Formation (Fig. 4d). These observations suggest that the
458 Tordillo Formation was proximal to the basin and constituted the main source of the Upper
459 Jurassic zircon population in the Colorado Strata.

Another possibility for the source of the analyzed granitic boulder could be recycling of either the Abanico Formation or the Neuquén Group (and their equivalents in Chile). The latter was deposited during the Late Cretaceous contractional deformation that led to the evolution of the back-arc Nequén Basin into a foreland basin (Cobbold and Rossello, 2003; Di Giulio et al., 2012; Ramos and Folguera, 2005; Tunik et al., 2010). However, the Neuquén Group usually exhibits U/Pb zircon ages from the Upper Cretaceous (Di Giulio et al., 2012; Tunik et al., 2010; Willner et al., 2005), which are not observed in the analyzed sandy sample from the Colorado Strata Unit.

Likewise, the absence of U/Pb zircon ages in the synorogenic unit corresponding to the age of the Abanico Formation suggests discarding this unit as a source. Nevertheless, the clastic composition of the synorogenic deposits is very similar to the volcanic composition of the Abanico Formation. Moreover, the Abanico Formation usually lacks of zircon grains given its predominantly tholeiitic composition. Furthermore, based on studies performed farther north (Charrier et al., 2009 and references therein) and the crystallization and cooling ages of the La Gallina and Río Negro plutons, the deformation in the Abanico Formation is constrained between approximately 20 and 3 Ma, i.e., younger than the maximum depositional age of the Colorado Strata Unit. Therefore, the Abanico Formation was likely a clastic source to the synorogenic deposits despite the lack of zircon U/Pb ages belonging to the range of ages of this unit.

The provenance of the minor Miocene zircon population (*ca.* 7 Ma) of the upper section of the synorogenic deposits could be derived from volcanic rocks such as those identified in the eastern part of the study region and farther east, with ages spanning between *ca.* 17 and 5 Ma (Combina and Nullo, 2011; Silvestro and Kraemer, 2005). The westward growth

strata observed in the Colorado Strata Unit also support a source from the east. Nevertheless, the Río Negro pluton, situated in the core of the Colorado Anticline a few kilometers west of the El Novillo thrust (Fig. 5a) is likely a source because its U/Pb zircon ages approximate this Miocene population despite the younger apatite U/Th-He ages obtained (*ca.* 3.8 Ma). The exhumation of these plutons may have begun earlier than the timing indicated by their apatite U/Th-He ages due to the low temperatures recorded by this thermochronometer.

Therefore, the Colorado Strata Unit was sourced mainly from the east and likely sourced from the Abanico Formation and the Río Negro pluton due to the activity of the Colorado Anticline and El Novillo thrust. There is no evidence for a relevant sedimentary input from either the western Principal Cordillera or farther west from the Coastal Cordillera. It is unlikely that incipient rivers west of the Colorado Anticline drained from the west to the basin. In contrast, it is likely that incipient rivers passed through the western Principal Cordillera draining to the west, as occurs at the present. In this scenario, the watershed could have been located farther to the east of the Debia and Valley Grande Anticlines, most likely east of the present-day drainage divide.

To summarize, the structural configuration in relation to the Colorado Strata Unit and the temporal relationship of deformation and deposition reveal that the synorogenic deposits developed in a basin enclosed by the Colorado anticline to the west and the Debia anticline to the east, forming a piggy-back basin system.

5.2 Synthesis of the Cenozoic evolution of the axial region and regional comparisons

Our results allow us to reconstruct the local evolution from the Miocene to the Present, which can be expanded to the north up to 35°S, where deposits with similar ages to the Colorado Strata Unit have been reported (González, 2008, Mosolf et al., 2011).

Fig. 9 here

Contractional deformation started in the western Principal Cordillera during the early Miocene with the inversion of the Abanico Basin and the onset of deformation along the western edge of the Malargüe FTB, represented by the Colorado, Valle Grande and Debia anticlines in the study region (Fig. 9a). Along with this evolution, the Colorado Strata Unit basin likely began to be filled during the first contractional event in the early Miocene, as evidenced by the growth strata that developed at the base of the sequence associated with the growth of the Debia anticline (Fig. 9a).

Following the in-sequence contractional deformation evolution proposed for this Andean region (Kozlowsky et al., 1993; Manceda and Figueroa, 1995; Silvestro and Kraemer, 2005), shortening has occurred in the Malargüe FTB since *ca.* 18-16 Ma (Fig. 9b) (*cf.* Mescua et al., 2014). Subsequently, several depocenters accumulated synorogenic sediments that were progressively deformed as shortening migrated to the east (Silvestro and Atencio, 2009; Silvestro and Kraemer, 2005). Although we do not have analytical evidence supporting this hypothesis during this stage, deposition continued in the Colorado Basin, and it is very likely that the erosion of the uplifting eastern zones supplied the sediments to this depocenter.

Between the late Miocene and the early Pleistocene, deformation was characterized by the development of both out-of-sequence and in-sequence thrusting that occurred simultaneously in the internal and external regions of the Andean orogen, respectively (Fig. 9c). In the axial region of the Principal Cordillera, thrusting and folding were associated with structures such as the El Novillo and Llolli thrusts, as well as the Calabozos thrust system, which deformed the synorogenic deposits and tilted the Abanico Formation to the west (Fig. 9c). This evolution, with the exception of the Calabozos thrust system, ended with the deposition of the Cola de Zorro Formation, which sealed the deformed sequences. However, the in-sequence thrusting is associated with the maximum expansion of the deformation toward the foreland, producing the uplift of the San Rafael Block and the broken foreland (Fig. 9c) (see Ramos et al., 2014). The origin of the out-of-sequence deformation and its implications are discussed in the next section.

The out-of-sequence thrusting episode was followed by the emplacement of the volcanic arc and the construction of the Peteroa-Azufre stratovolcano and Calabozos caldera (Fig. 9d), indicating the beginning of the current volcanic arc along the southern Central Andes. Thereafter, the shortening became concentrated in the internal zone to the south of the study region, as evidenced by faults such as the Calabozos thrusts system and the development of the Guañacos fold-and-thrust belt farther south (Folguera et al., 2006a). In contrast, the retro-arc region has experienced extensional tectonics since the Early Pleistocene, and extension controlled the structural array and location of the volcanic centers that erupted the large basaltic flows of the Payenia volcanic field (Fig. 9d).

5.3 Kinematics context of the inner mountain belt.

The study area, particularly the Calabozos caldera, has been described as the northernmost tip of the NNW-trending extensional Las Loicas Trough, which has been proposed to have developed during the steepening of the subducting slab in the Quaternary after a period of slab shallowing during the Miocene (Folguera et al., 2008; Ramos et al., 2014). However, field observations made in our study area show that there is no evidence of normal faulting in the area, with the exception of several minor, local-scale normal faults in the core of volcanic edifices belonging to the Calabozos caldera (Fig. 1c) (Grunder and Mahood, 1988; Grunder, 1987; Grunder et al., 1987; Hildreth et al., 1984). Therefore, the region does not exhibit evidence for extending the extensional Las Loicas Trough to the current arc region.

In contrast, we observe an almost continuous contractional setting from the late Miocene to the present in this zone. Therefore, extensional tectonics did not affect the arc region during the Quaternary, but the area was affected by across-strike shortening. Several studies have noted that the tectonic regime of the axial zone of this part of the Southern Central Andes has been mainly transcurrent based on seismological focal mechanisms aligned with the regional El Fierro Thrust System (Fig. 1b) (*e.g.*, Farías et al., 2010; Spagnuotto et al., 2014, Giamabiagi et al., 2014). In contrast, finite deformation estimates based on kinematic modeling of GPS data indicate shortening parallel to the plate convergence vector (~N78ºE, see Fig. 1a and b) for the Southern Central Andes (*cf.*, Métois et al., 2012; and reference therein).

The apparent disagreement between GPS-based kinematic models and seismological focal mechanisms can be explained by the high obliquity (45-50º) between the plate convergence

vector and the El Fierro Thrust System with recorded strike-slip earthquakes (Fig. 1b). In contrast, structures more orthogonal to the plate convergence vector will favor shortening rather than strike-slip.

Nevertheless, shortening in the axis of the belt can only be achieved when vertical stress related to the height and weight of the mountain belt is less than the horizontal stress, as proposed for other zones of the Andes (*e.g.*, Dalmayrac and Molnar, 1981; Farías et al., 2005; 2010). In this way, shortening related to the out-of-sequence thrusting in the study region is likely related to both the high orthogonality of the structural systems with respect to the plate convergence vector and to the minor resistance to shortening produced by the minor height of the mountain belt and the removal of material via erosion of the uplifted mountain belt. The former suggests strain partitioning in the axial zone in this part of the Andean Cordillera.

Likewise, the tectonic setting proposed here for the current axial region differs from the extensional setting that the retro-arc experienced during the subduction slab steepening stage (Ramos et al., 2014 and references therein). This observation also suggests strain partitioning between the axial zone with respect to the eastern mountain belt and foreland. In this way, shortening, strike-slip and extension could coexist in this part of the Andes.

Beyond the objective of this study, the origin of the strain partitioning between strike-slip/shortening in the axial region and the extensional setting in the retro-arc can be addressed to the effects of the shallowing and steepening of the subducting plate proposed for this Andean region during the latest Cenozoic (Kay et al., 2006; Ramos and Kay 2006). This type of process would produce changes in the thermal structure of the lithosphere, thus

affecting the deformation behavior of the overriding plate (Gutscher, 2002). Along this line, we infer that these thermal changes during slab steepening produced different effects in the arc and retro-arc regions due to the differences in the rheology, lithospheric thickness, crustal structure, etc. However, further work is necessary to demonstrate this hypothesis. At a minimum, the extensional deformation did not affect the current axial/arc region at 35º30'S, as previously extrapolated to this region.

5.4 Out-of-sequence thrusting in the Southern Central Andes

Out-of-sequence thrusting in the inner parts of mountain belts has been widely documented in orogenic systems worldwide, including the southern Central Andes. In fact, north of the study region, out-of-sequence thrusting in the mountain belt ended by the Pliocene in the Aconcagua fold-and-thrust belt (33°-34ºS) (Giambiagi and Ramos, 2002; Giambiagi et al., 2003). Only transcurrent deformation has occurred since then in the axial zone (Farías et al., 2010, Giambiagi et al., 2014). In contrast, south of the study region, the Guañacos fold-and-thrust belt (37°S) experienced contractional deformation that began in the late Miocene and has continued until the Present (Folguera et al., 2006a). Thus, a regional-scale out-of-sequence event began during the late Miocene in the southern Central Andes. This event ended first north of the study region and has continued to the Present south of 35ºS.

The origin of out-of-sequence events can be approached from the Coulomb wedge model (Davis et al., 1983), where out-of-sequence thrusting is an integral part of the formation of thrust belts because it maintains the critical wedge taper (Morley, 1988). Out-of-sequence thrusting in the wedge model can be triggered by the loss of the taper, which can be caused by either erosion, the elongation of the wedge through foreland propagation of the thrust

belt or local obstacles that impede the propagation of in-sequence thrusts (Morley, 1988). Additionally, an increase in the friction along the taper may also produce out-of-sequence thrusting (Dahlen et al., 1984; Davis et al., 1983).

The late Miocene out-of-sequence thrusting event that affected the southern Central Andes was concurrent with large-magnitude rates of surface uplift between, at least, 33º and 35ºS, which can be directly related to a coeval increase in shortening rates (*cf.* Giambiagi et al., 2003; 2014; Farías et al., 2008; 2010). Furthermore, an increase in the regional slope of the mountain range produced by surface uplift would enhance material discharge from the orogen by increasing erosional rates, a process that will also favor the development of out-of-sequence thrusts. Thus, the triggering of out-of-sequence thrusting in the southern Central Andes can be ascribed to the increasing shortening rates, but this process was undoubtedly also favored by mass transfer out from the mountain belt by erosion.

An increase in shortening rates may be a result of an increase in friction along the interplate contact due to the subduction of a more buoyant heterogeneity on the subducting slab. Along this line, Folguera and Ramos (2009) proposed the subduction of an oceanic rise related to the Mocha Fracture Zone beginning in the late Pliocene to explain a Pliocene-Pleistocene out-of-sequence thrusting event between 36 and 38ºS. However, the beginning of the out-of-sequence thrusting event reported in our study began at least in the late Miocene, that is, approximately coeval with thrusting to the north to 33º (*e.g.*, Giambiagi et al., 2003; Farías et al., 2010) and farther south in the Guañacos fold-and-thrust belt between 37ºS and 37º30'S (Folguera et al., 2006a; Rojas Vera et al., 2014). Hence, the out-of-sequence thrusting event was a regional event in the southern Central Andes, extending along more than 500 km between 33° and 37°30'S. In addition, it began in the late

Miocene, preceding the collision of the oceanic high proposed by Folguera and Ramos (2009). Therefore, it is unlikely that this oceanic feature controlled this thrusting event, even though it could have affected the thrusting in the Guañacos fold-and-thrust belt until the early Pleistocene. Therefore, another mechanism must be responsible for this event.

Therefore, considering the likely role of erosion on the development of out-of-sequence thrusting, such a mechanism indirectly implies a control exerted by climate. In fact, this would be the case when considering the fact that the out-of-sequence thrusting lasted longer in the south of the mountain belt than in the north. South of 33ºS, precipitation rates increase significantly, the effects of mountain glaciations in the range become progressively larger, and there is a southward increase in long-term erosion rates (Carretier et al., 2014, 2012; Farías et al., 2008; 2012). To the south, the more intense erosion is a more efficient mechanism for sustaining the development of out-of-sequence thrusts through time.

6 Summary and Conclusions

The structural, sedimentological and geochronological studies in this portion of the arc in the southern Central Andes allow us to demonstrate that this region has experienced contractional deformation from at least the late Miocene to the Present. This deformation was characterized by the development of a piggy-back basin in the latest Miocene. Afterward, the region experienced shortening associated with an out-of-sequence thrusting event that affected the inner part of the Malargüe FTB from the Pliocene until the Present.

The southward increases in the rates of precipitation and erosion are a likely, efficient mechanism for material removal from the steepest zone of the orogen, which triggered the out-sequence thrusting in the internal region of the Andes Cordillera. More intense erosion

and subsequent out-of-sequence thrusting illustrate the feedback between the surface processes and tectonics present along the southern Central Andes.

Acknowledgements

This research was supported by the FONDECYT grants 1120272 and 11085022. F. Tapia's doctoral study at the Universidad de Chile has been supported by Doctoral CONICYT Scholarship. This study was also supported by the Institute de Recherche pour le Développement (IRD-France). We thank R. Charrier, S. Calderón, J. Valenzuela and J. Cortés for field support. M. P. Rodríguez and S. Brichau are thanked for the numerous useful discussions regarding the geology of the Andes. The authors kindly thank M. Muñoz for detailed review and constructive comments.

References

Carretier, S., Regard, V., Vassallo, R., Aguilar, G., Martinod, J., Riquelme, R., Pepin, E., Charrier, R., Herail, G., Farías, M., Guyot, J.-L., Vargas, G., Lagane, C., 2012. Slope and climate variability control of erosion in the Andes of central Chile. Geology 41, 195–198.

Carretier, S., Tolorza, V., Rodriguez, M.P., Pepin, E., Aguilar, G., Regard, V., Martinod, J., Riquelme, R., Bonnet, S., Brichau, S., Herail, G., Pinto, L., Farías, M., Charrier, R., Guyot, J.L., 2014. Erosion in the Chilean Andes between 27 S and 39 S: tectonic, climatic and geomorphic control. Geol. Soc. London, Spec. Publ. 399. doi: 10.1144/SP399.16

Charrier, R., 1979. El Triásico de Chile y regiones adyacentes en Argentina: Una reconstrucción paleogeográfica y paleoclimática. Comunicaciones 26, 1–47.

676 Charrier, R., Wyss, A.R., Flynn, J.J., Swisher III, C.C., Norell, M.A., Zapatta, F., Mckenna, M.C.,
677 Novacek, M.J., 1996. New evidence for Late Mesozoic-Early Cenozoic evolution of the
678 Central Chile. J. South Am. Earth Sci. 9, 393–422.

679 Charrier, R., Baeza, O., Elgueta, S., Flynn, J., Gans, P., Kay, S., Muñoz, N., Wyss, A., Zurita, E.,
680 2002. Evidence for Cenozoic extensional basin development and tectonic inversion south of
681 the flat-slab segment, southern Central Andes, Chile (33°–36°S.L.). J. South Am. Earth Sci.
682 15, 117–139.

683 Charrier, R., Pinto, L., Rodríguez, M.P., 2007. Tectonostratigraphic evolution of the Andean
684 Orogen in Chile, in: Moreno, T., Gibbons, W. (Eds.), The Andes of Chile. Geological Society
685 of London, pp. 21–114.

686 Charrier, R., Farías, M., Maksaev, V., 2009. Evolución tectónica, paleogeográfica y metalogénica
687 durante el Cenozoico en los Andes de Chile norte y central e implicaciones para las regiones
688 adyacentes de Bolivia y Argentina. Rev. la Asoc. Geológica Argentina 65, 5–35.

689 Charrier, R., Ramos, V. A., Tapia, F., Sagripanti, L., 2014. Tectono-stratigraphic evolution of the
690 Andean Orogen between 31 and 37 S (Chile and Western Argentina). Geol. Soc. London,
691 Spec. Publ 399, doi: 10.1144/SP399.20

692 Cobbold, P., Rossello, E., 2003. Aptian to recent compressional deformation, foothills of the
693 Neuquén Basin, Argentina. Mar. Pet. Geol. 20, 429–443.

694 Combina, A.M., Nullo, F., 2011. Ciclos tectónicos , volcánicos y sedimentarios del Cenozoico del
695 sur de Mendoza-Argentina (35°-37°S y 69°30'W). Andean Geol. 38, 198–218.

696 Dahlen, F. A., Suppe, J., Davis, D., 1984. Mechanics of fold-and-thrust belts and accretionary
697 wedges: Cohesive Coulomb Theory. J. Geophys. Res. 89, 10087.

698 Dalmayrac, B., Molnar, P., 1981. Parallel thrust and normal faulting in Peru and constraints on the
699 state of stress. Earth Planet. Sci. Lett. 55, 473–481.

700 Davis, D., Suppe, J., Dahlen, F.A., 1983. Mechanics of fold-and-thrust belts and accretionary
701 wedges. J. Geophys. Res. Solid Earth 88, 1153–1172.

702 Di Giulio, A., Ronchi, A., Sanfilippo, A., Tiepolo, M., Pimentel, M., Ramos, V. A., 2012. Detrital
703 zircon provenance from the Neuquén Basin (south-central Andes): Cretaceous geodynamic
704 evolution and sedimentary response in a retroarc-foreland basin. Geology 40, 559–562.

705 Drake, R.E., 1976. Chronology of cenozoic igneous and tectonic events in the central Chilean
706 Andes — latitudes 35° 30′ to 36°S. J. Volcanol. Geotherm. Res. 1, 265–284.

707 Espizúa, L.E., 2005. Holocene glacier chronology of Valenzuela Valley, Mendoza Andes,
708 Argentina. The Holocene 15, 1079–1085.

709 Farías, M., Charrier, R., Comte, D., Martinod, J., Hérail, G., 2005. Late Cenozoic deformation and
710 uplift of the western flank of the Altiplano: Evidence from the depositional, tectonic, and
711 geomorphologic evolution and shallow seismic activity (northern Chile at 19°30'S). Tectonics
712 24, TC4001.

713 Farías, M., Charrier, R., Carretier, S., Martinod, J., Fock, A., Campbell, D., Cáceres, J., Comte, D.,
714 2008. Late Miocene high and rapid surface uplift and its erosional response in the Andes of
715 central Chile (33°-35°S). Tectonics 27, doi:10.1029/2006TC002046.

716 Farías, M., Tapia, F., Comte, D., 2009. La Falla Calabozos: Un cabalgamiento activo en la alta
717 cordillera de Curicó, in: XII Congreso Geológico Chileno. Santiago, Chile, electronic abstract.

718 Farías, M., Comte, D., Charrier, R., Martinod, J., David, C., Tassara, A., Tapia, F., Fock, A., 2010.
719 Crustal-scale structural architecture in central Chile based on seismicity and surface geology:
720 Implications for Andean mountain building. Tectonics 29. doi:10.1029/2009TC002480.

721 Farías, M., Charrier, R., Carretier, S., Tapia, F., Astaburuaga, D., Puratich, J., Rodríguez, M.P.,
722 Urresty, C., Garrido, G., 2012. Contribución de largo-plazo de la segmentación climática en
723 Chile Central a la construcción Andina, in: XIII Congreso Geológico Chileno. Antofagasta,
724 Chile, pp. 191–193.

725 Fock, A., Charrier, R., Farías, M., Muñoz, M.A., 2006. Fallas de vergencia oeste en la Cordillera
726 Principal de Chile Central: Inversión de la cuenca de Abanico (33°-34°S), in: Hongn, F.,
727 Becchio, R., Seggiario, R (Eds), XII Reunión sobre microtectónica y geología estructural.
728 Rev. Asoc. Geológica Argentina, Serie D, Publicación Especial 6, 48-55.

729 Folguera, A., Ramos, V. A., 2009. Collision of the Mocha fracture zone and a <4 Ma old wave of
730 orogenic uplift in the Andes (36 -38 S). Lithosphere 1, 364–369.

731 Folguera, A., Ramos, V. A., Hermanns, R.L., Naranjo, J., 2004. Neotectonics in the foothills of the
732 southernmost central Andes (37°-38°S): Evidence of strike-slip displacement along the
733 Antiñir-Copahue fault zone. Tectonics 23, doi: 10.1029/2003TC001533.

734 Folguera, A., Ramos, V.A., González Díaz, E.F., Hermanns, R., 2006a. Miocene to Quaternary
735 deformation of the Guañacos fold-and-thrust belt in the Neuquén Andes between 37°S and
736 37°30′S. in: Kay, S.M., Ramos, V.A. (Eds.), Evolution of an Andean Margin: A Tectonic and
737 Magmatic View from the Andes to the Neuquen Basin (35°-39°S Lat). Geol. Soc. Am. Spec.
738 Pap. 407, 247–266.

739 Folguera, A., Zapata, T., Ramos, V.A., 2006b. Late Cenozoic extension and the evolution of the
740 Neuquén Andes, in: Kay, S.M., Ramos, V.A. (Eds.), Evolution of an Andean Margin: A
741 Tectonic and Magmatic View from the Andes to the Neuquen Basin (35°-39°S Lat).
742 Geological Society of America, Special Papers 407, pp. 267–285.

743 Folguera, A., Introcaso, A., Giménez, M., Ruiz, F., Martinez, P., Tunstall, C., García Morabito, E.,
744 Ramos, V. A., 2007a. Crustal attenuation in the Southern Andean retroarc (38°–39°30′ S)
745 determined from tectonic and gravimetric studies: The Lonco-Luán asthenospheric anomaly.
746 Tectonophysics 439, 129–147.

747 Folguera, A., Ramos, V. A., Zapata, T., Spagnuolo, M.G., 2007b. Andean evolution at the
748 Guañacos and Chos Malal fold and thrust belts (36°30′–37°S). J. Geodyn. 44, 129–148.

749 Folguera, A., Bottesi, G., Zapata, T., Ramos, V. A., 2008. Crustal collapse in the Andean backarc
750 since 2 Ma: Tromen volcanic plateau, Southern Central Andes (36°40′–37°30′S).
751 Tectonophysics 459, 140–160.

752 Folguera, A., Naranjo, J.A., Orihashi, Y., Sumino, H., Nagao, K., Polanco, E., Ramos, V.A., 2009.
753 Retroarc volcanism in the northern San Rafael Block (34 degrees-35 degrees 30 ’ S), southern
754 Central Andes: Occurrence, age, and tectonic setting. J. Volcanol. Geotherm. Res. 186, 169–
755 185.

756 Folguera, A., Rojas Vera, E., Bottesi, G., Zamora Valcarce, G., Ramos, V. A., 2010. The Loncopué
757 Trough: A Cenozoic basin produced by extension in the southern Central Andes. J. Geodyn.
758 49, 287–295.

759 Folguera, A., Orts, D., Spagnuolo, M., Vera, E.R., Litvak, V., Sagripanti, L., Ramos, M.E., Ramos,
760 V.A., 2011. A review of Late Cretaceous to Quaternary palaeogeography of the southern
761 Andes. Biol. J. Linn. Soc. 103, 250–268.

762 Folguera, A., Alasonati Tašárová, Z., Götze, H.-J., Rojas Vera, E., Giménez, M., Ramos, V. A.,
763 2012. Retroarc extension in the last 6 Ma in the South-Central Andes (36°S–40°S) evaluated
764 through a 3-D gravity modelling. J. South Am. Earth Sci. 40, 23–37.

765 García Morabito, E., Folguera, A., 2005. El alto de Copahue-Pino Hachado y la fosa de Loncopué:
766 un comportamiento tectónico episódico, Andes neuquinos (37°-39°S). Rev. Asoc. Geológica
767 Argentina 60, 742–761.

768 Giambiagi, L., Ramos, V.A., 2002. Structural evolution of the Andes in a transitional zone between
769 flat and normal subduction (33°30′–33°45′S), Argentina and Chile. J. South Am. Earth Sci. 15,
770 101–116.

771 Giambiagi, L., Ramos, V.A., Godoy, E., Alvarez, P.P., Orts, S., 2003. Cenozoic deformation and
772 tectonic style of the Andes, between 33 degrees and 34 degrees south latitude. Tectonics 22,
773 1041.

774 Giambiagi, L.B., Bechis, F., Garcia, V., Clark, A.H., 2008. Temporal and spatial relationships of
775 thick- and thin-skinned deformation: A case study from the Malargue fold-and-thrust belt,
776 southern Central Andes. Tectonophysics 459, 123–139.

777 Giambiagi, L., Ghiglione, M., Cristallini, E., Bottesi, G., 2009. Kinematic models of
778 basement/cover interaction: Insights from the Malargüe fold and thrust belt, Mendoza,
779 Argentina. J. Struct. Geol. 31, 1443–1457.

780 Giambiagi, L.B., Tassara, A., Mescua, J., Tunik, M., Alvarez, P.P., Godoy, E., Hoke, G.D., Pinto,
781 L., Spagnotto, S., Porras, H., Tapia, F., Jara, P., Bechis, F., Garcia, V.H., Suriano, J.,
782 Moreiras, S.M., Pagano, S.D., 2014. Evolution of shallow and deep structures along the
783 Maipo-Tunuyan transect (33 40'S): from the Pacific coast to the Andean foreland, in:
784 Sepúlveda, S. A., Giambiagi, L. B., Moreiras, S. M., Pinto, L., Tunik, M., Hoke, G. D., Farías,
785 M. (Eds), Geodynamic Processes in the Andes of Central Chile and Argentina. Geol. Soc.
786 London, Spec. Publ. 399.

787 Godoy, E., Yáñez, G., Vera, E., 1999. Inversion of an Oligocene volcano-tectonic basin and
788 uplifting of its superimposed Miocene magmatic arc in the Chilean Central Andes: First
789 seismic and gravity evidences. Tectonophysics 306, 217–236.

790 González, A., 2008. Análisis estructural entre los valles del río Tinguiririca y Teno, Cordillera
791 Principal de Chile Central: Microsismisidad y Geología Superficial. Unpublished thesis.
792 Universidad de Chile.

793 González Díaz, E.F., 1972. Descripción Geológica de la Hoja 27d, San Rafael, Provincia de
794 Mendoza. Serv. Geológico Min. Argentino. Boletín 132, 1–127.

795 González, O., Vergara, M., 1962. Reconocimiento geologico de la Cordillera de los Andes entre los
796 paralelos 35° y 38° S. Inst. Investig. Geológicas 1.

797 Grunder, A.L., 1987. Low δ18O silicic volcanic rocks at the Calabozos caldera complex, southern
798 Andes. Contrib. to Mineral. Petrol. 95, 71–81.

799 Grunder, A.L., Thompson, J.M., Hildreth, W., 1987. The hydrothermal system of the Calabozos
800 caldera, central Chilean Andes. J. Volcanol. Geotherm. Res. 32, 287–298.

801 Grunder, A.L., Mahood, G.A., 1988. Physical and chemical models of zoned silicic magmas. The
802 Loma Seca Tuff and Calabozos Caldera, southern Andes. J. Petrol. 29, 831–867.

803 Gulisano, C., Gutiérrez Pleimling, A.R., 1995. The Jurassic of the Neuquén Basin: Mendoza
804 Province. Guía de Campo, in: Asociación Geológica Argentina, Special Publication, Vol. 159.
805 Argentina. p. 103.

806 Gutscher, M.-A., 2002. Andean subduction styles and their effect on thermal structure and interplate
807 coupling. J. South Am. Earth Sci. 15, 3–10.

808 Hildreth, W., Grunder, A., Drake, R., 1984. The Loma Seca Tuff and the Calabozos caldera: A
809 major ash-flow and caldera complex in the southern Andes of central Chile. Geol. Soc. Am.
810 Bull. 95, 45–54.

811 Kay, S.M., Godoy, E., Kurtz, A., 2005. Episodic arc migration, crustal thickening, subduction
812 erosion, and magmatism in the south-central Andes. Geol. Soc. Am. Bull. 117, 67.

813 Kay, S. M., Burns, M., Copeland, P., 2006. Upper Cretaceous to Holocene Magmatismover the
814 Neuquén basin: evidence for transient shallowing of the subduction zone under the Neuquén
815 Andes (36°S to 38°S latitude), in: Kay, S. M., and Ramos, V. A.(Eds.), Evolution of an
816 Andean margin: A tectonic and magmatic view form the Andes to the Neuquén Basin (35°S-
817 39°S lat): Geological Society of America Special Papers 407. pp.19-60.

818 Kozlowsky, E., Manceda, R., Ramos, V.A., 1993. Estructura, in: Ramos, V.A. (Ed.), Geología y
819 Recursos Naturales de La Provincia de Mendoza. Relatorio del XII Congreso Geológico
820 Argentino. Mendoza, pp. 235–256.

821 Litvak, V.D., Folguera, A., 2008. Determination of an arc-related signature in Late Miocene
822 volcanism over the San Rafael Block, Southern Central Andes (34°30'-37°S) Argentina: the

Payenia shallow subducting zone, in: 7° International Symposium on Andean Geodynamics. Niza, pp. 289–291.

Manceda, R., Figueroa, D., 1995. Inversion of the Mesozoic Neuquén Rift in the Malargüe Fold and Thrust Belt, Mendoza, Argentina, in: Tankard, A.J., Suárez S., R., Welsink, H.J. (Eds.), Petroleum Basin of South America. AAPG Memoir 62, pp. 369–382.

Mescua, J.F., Giambiagi, L.B., Tassara, A., Gimenez, M., Ramos, V.A., 2014. Influence of pre-Andean history over Cenozoic foreland deformation: Structural styles in the Malargue fold-and-thrust belt at 35 S, Andes of Argentina. Geosphere 1–25.

Métois, M., Socquet, a., Vigny, C., 2012. Interseismic coupling, segmentation and mechanical behavior of the central Chile subduction zone. J. Geophys. Res. Solid Earth 117.

Morley, C.K., 1988. Out-of-Sequence Thrusts. Tectonics 7, 539–561.

Mosolf, J.G., Gans, P.B., Wyss, A.R., Cottle, J.M., 2011. Detailed geologic field mapping and radiometric dating of the Abanico Formation in the Principal Cordillera, central Chile: Evidence of protracted volcanism and implications for Cenozoic tectonics, in: AGU Fall Meeting Abstracts. p. abstract #V13C–2623.

Mpodozis, C., Ramos, V.A., 1989. The Andes of Chile and Argentina, in: Ericksen, G.E. (Ed.), Geology of the Andes and Its Relation to Hydrocarbon and Mineral Resources. Earth Sci. Ser, pp. 59–90.

Naranjo, J., Haller, M., 2002. Erupciones holocenas principalmente explosivas del volcán Planchón, Andes del sur (35°15'S). Rev. geológica Chile 29, 93–113.

843 Naranjo, J., Haller, M., Ostera, H., Pesce, A.H., Sruoga, P., 1999. Geología y peligros del Complejo
844 Volcánico Planchón-Peteroa, Andes del Sur (35°15'S), Región del Maule, Chile-Provincia de
845 Mendoza, Argentina. Serv. Nac. Geol. y Minería, Bol. 52, 55p.

846 Pose, F.A., Spagnuolo, M.G., Folguera, A., 2005. Modelo para la variación del volumen orogénico
847 andino y acortamientos en el sector 20°-46°S. Rev. la Asoc. Geológica Argentina 60, 724–
848 730.

849 Ramos, V.A., 2000a. Las Provincias Geológicas del Territorio Argentino, in: Caminos, R. (Ed.),
850 Geología Argentina. Instituto de Geología y Recursos Minerales, Anales 29(3), pp. 41-96.

851 Ramos, V.A., 2000b. The Southern Central Andes, in: Cordani, U.G., Milani, E.J., Thomas Fhilo,
852 A., Campos, A. (Eds.), Tectonic Evolution of South America. 31° International Geological
853 Congress, Rio de Janeiro, Río de Janeiro, pp. 561–604.

854 Ramos, V.A., Folguera, A., 2005. Tectonic evolution of the Andes of Neuquén: constraints derived
855 from the magmatic arc and foreland deformation, in: Veiga, G., Spalletti, J., Howell, J.,
856 Schwarz, E., (Eds), The Neuquén Basin: A case study in sequence stratigraphy and basin
857 dinamics. Geol. Soc. London, Spec. Publ. 252, 15–35.

858 Ramos, V.A., Kay, S.M., 2006. Overview of the tectonic evolution of the southern Central Andes of
859 Mendoza and Neuquén (35°–39°S latitude), in: Kay, S.M., Ramos, V.A. (Eds.), Evolution of
860 an Andean Margin: A Tectonic and Magmatic View from the Andes to the Neuquen Basin
861 (35°-39°S Lat). Geological Society of America Special Papers 407. pp. 1–17.

862 Ramos, V.A., Folguera, A., 2011. Payenia volcanic province in the Southern Andes: An appraisal of
863 an exceptional Quaternary tectonic setting. J. Volcanol. Geotherm. Res. 201, 53–64.

Ramos, V. A., Litvak, V.D., Folguera, A., Spagnuolo, M., 2014. An Andean tectonic cycle: From crustal thickening to extension in a thin crust (34°–37°SL). Geosci. Front. 1–17.Rojas Vera, E. a., Folguera, A., Zamora Valcarce, G., Bottesi, G., Ramos, V. a., 2014. Structure and development of the Andean system between 36° and 39°S. J. Geodyn. 73, 34–52.

Rojas Vera, E.A., Folguera, A., Valcarce, G.Z., Giménez, M., Ruiz, F., Martínez, P., Bottesi, G., Ramos, V.A., 2010. Neogene to Quaternary extensional reactivation of a fold and thrust belt: The Agrio belt in the Southern Central Andes and its relation to the Loncopué trough (38°–39°S). Tectonophysics 492, 279–294.

Servicio Geológico Minero Argentino, 1997. Mapa geológico de la Republica Argentina, escala 1:2.500.000, Buenos Aires, Argentina.

Servicio Nacional de Geología y Minería, 2002. Mapa geológico de Chile, escala 1:1.000.000, Mapa M61.

Silvestro, J., Kraemer, P., 2005. Evolución de las cuencas sinorogénicas de la Cordillera Principal entre 35°-36° S, Malargüe. Rev. la Asoc. Geológica Argentina 60, 627–643.

Silvestro, J., Atencio, M., 2009. La cuenca cenozoica del río Grande y Palauco: edad, evolución y control estructural, faja plegada de Malargüe. Rev. la Asoc. Geológica Argentina 65, 154–169.

Spagnuolo, M.G., Litvak, V.D., Folguera, A., Bottesi, G., Ramos, V.A., 2012. Neogene magmatic expansion and mountain building processes in the southern Central Andes, 36–37°S, Argentina. J. Geodyn. 53, 81–94.

Spagnotto, S., Nacif, S., Yacante, G., Giambiagi, L.B., 2014. Sismo Mw=6.0 del 7 de Junio del 2012 y aftershocks en las inmediaciones del Complejo Volcánico San Pedro-Pellado, Linares, Chile, in: XIX Congreso Geológico Argentino. Cordoba.

886 Tassara, A., 2005. Interaction between the Nazca and South American plates and formation of the
887 Altiplano–Puna plateau: Review of a flexural analysis along the Andean margin (15°–34°S).
888 Tectonophysics 399, 39–57.

889 Tassara, A., Echaurren, A., 2012. Anatomy of the Andean subduction zone: three-dimensional
890 density model upgraded and compared against global-scale models. Geophys. J. Int. 189, 161–
891 168.

892 Tunik, M., Folguera, A., Naipauer, M., Pimentel, M., Ramos, V.A., 2010. Early uplift and orogenic
893 deformation in the Neuquén Basin: Constraints on the Andean uplift from U–Pb and Hf
894 isotopic data of detrital zircons. Tectonophysics 489, 258–273.

895 Uliana, M.A., Biddle, J., Cerdan, J.J., 1989. Mesozoic Extension and the Formation of Argentine
896 Sedimentary Basins, in: Tankard, A.J., Balkwill, H.R. (Eds.), Extensional Tectonics and
897 Stratigraphy of the North Atlantic Margins, vol.46. AAPG Memoir 46, pp. 599–614.

898 Uyeda, S., Kanamori, H., 1979. Back-arc opening and the mode of subduction. J. Geophys. Res. 84,
899 1049.

900 Willner, A.P., Thomson, S.N., Kröner, A., Wartho, J.-A., Wijbrans, J.A., Hervé, F., 2005. Time
901 Markers for the Evolution and Exhumation History of a Late Palaeozoic Paired Metamorphic
902 Belt in North–Central Chile (34°–35°30′S). J. Petrol. 46, 1835–1858.

903 Figure 1: (a) Tectonic framework of the Andean margin. The arrows indicate the absolute
904 plate motion; the dashed line delineates the Neuquén Basin margin; the filled black
905 rectangle shows the location of Figure 1b. (b) Simplified geologic map of the Chilean-
906 Argentinean Andean margin between 33° and 37°S showing major structures and main
907 lithological units (Taken from Farías et al., 2010; Folguera et al., 2006b; Giambiagi et al.,

2003, 2008, 2009, 2012; Servicio Geológico Minero Argentino, 1997; Servicio Nacional de Geología y Minería, 2002). Moreover, are indicated the focal mechanism of the crustal shallow earthquake of the last years. The focal mechanism are taken by Harvard CMT and Earthquake Program of the USGS. The black rectangle shows the location of the Figure 2a. AFTB: Aconcagua fold-and-thrust belt; CC: Calabozos caldera; CHFTB: Chos Malal fold-and-thrust belt; DV: Domuyo volcano; FTS: El Fierro Thrust System; GFTB: Guañacos fold-and-thrust belt; LLT: Las Loicas Trough; LT: Loncopue trough; MFTB: Malargüe fold-and-thrust belt; MC: Maule caldera;; PC: Palao caldera; TV: Tromen volcano; VC: Varvarco caldera. (c) Digital elevation model (DEM) of the study area showing the location of the samples and the Calabozos caldera. Morphology and location of the normal fault of the caldera was taken from Hildreth et al., 1984. The black rectangle indicates the location of the Figure 2a.

Figure 2: (a) Geological map of the study area. Circled numbers correspond to the following lithological and structural units: (1) Río Negro pluton; (2) Colorado anticline; (3) Novillo thrust; (4) Llolli thrust; (5) Valle Grande anticline; (6) Debia anticline; (7) Calabozos thrusts system; (8) Potrerillos pluton. Letters within black rectangles correspond to the following locations: (A) Novillo stream; (B) Cerro Las Yeguas; (C) Llolli ; (D) Cerro El Pellejo; (E) Debia creek; (F) Cerro Negro. (b) Concordia diagrams for U-Pb determinations by LA-MC-ICP-MS for the Potrerillos pluton. (c) and (d) Concordia diagrams for U-Pb determinations by CA-TIMS for the Río Negro and La Gallina plutons. Ellipses for U-Pb data at ±2σ error level.

Figure 3: Features of the Colorado Strata Unit. (a) Unconformity between Mesozoic rocks and the synorogenic deposits of the Colorado Strata in the western slope of the Valle

Grande valley. (b) Contact between the Colorado Strata and Vaca Muerta Formation in the Debia creek. The synorogenic deposits show growth strata. The white circle shows the scale. (c) Contact relationship between Auquilco Formation and Colorado Strata Unit in the northern slope of the Cerro Las Yeguas. (d) Cross stratification in sandstone. (e) Sand lens in a clast-supported conglomerate. (f) Intrusive clast and drying cracks in red siltstone of the synorogenic deposits. (g) Conglomerates with volcanic and sedimentary clasts. (See Figure 2a for location of the photographs).

Figure 4. Photomicrographs of sandstones from different stratigraphic units of the study area. (a-c) Samples from the Colorado Strata Unit at the Cerro Las Yeguas of red sandstones with plagioclase feldspars and lithic fragments. (d) Red sandstone of the Tordillo Formation from the eastern limb of the Valle Grande anticline. (e-f) Sandstone of the Colorado Strata Unit in the Debia creek. Pl: plagioclase feldspars; Qtz: quartz; Lv: volcanic lithic; Ls: sedimentary lithic.

Figure 5. (a) Schematic structural cross-sections of the study area showing the main structural features described in the text (see Fig. 2a for location). (b) Structural cross-section along the Debia creek showing the details of the deformation associated with the Calabozos thrusts system.

Figure 6. Geology of the Cerro Las Yeguas area. (a) Southward view of the disposition of the Colorado Strata Unit over the Mesozoic sequences. The double-head arrows show the western thickness growth of the synorogenic deposits. The image was taken from the Google Earth software. (b) Detailed view to west of the anticline along the Nevado river involving the synorogenic deposits. This fold is associated to the Llolli thrust deformation.

953 (c) View to the southern slope of the Colorado river valley where the synorogenic deposits
954 are repeated by the Llolli thrust. Unconformity over this thrust separates these deposits
955 from the Neogene sedimentary rocks of the Cola de Zorro Formation.

956 Figure 7. Main deformational features in the synorogenic deposits. (a) Aerial photograph
957 showing the main traces of the Calabozos thrusts system, the eastern border of the
958 Calabozos Caldera and location of the pictures in Figures 8b-8h. (b) Scarp associated with
959 the Calabozos thrusts system in the Debia creek area. (c) NS trending main faults and
960 related on echelon faults of the Calabozos thrusts system. (d) South view of the structural
961 arrangement of the Calabozos thrusts along the sag pond developed between the N30°E
962 trending echelon faults. (e) Deformation along the Debia creek showing the anticline
963 formed by the Calabozos thrusts system. The white circle shows the scale. (f) Northern
964 segment of the Calabozos thrusts system where only one branch can be recognized. (g)
965 Quaternary unconsolidated deposits with reverse offset produced by the southern segment
966 of the Calabozos thrusts system. (h) North view of the reverse main fault of the Calabozos
967 thrusts system affecting moraines and *roches moutonnés* in the northern slope of the Debia
968 creek.

969 Figure 8. (a) Partial stratigraphic section of the Colorado Strata Unit at the Cerro Las Yeguas
970 showing the main stratigraphic and sedimentary characteristics (See Figure 2a for location).
971 Diagrams of Concordia (left) and frequency histogram and relative probability (right) for the zircon
972 U-Pb age determinations of samples TA11-22A (b) and TA11-22B (c). Cathodoluminescence
973 images of representative zircons are also shown as inset in the right diagrams. (d) Field photograph
974 of the conglomerate and sandstone layers where the TA11-22A and TA11-22B samples were
975 collected.

Figure 9. Interpretative maps summarizing the evolution across the Andean region between 34° and 37°S. The evolution between 34° and 35°S is based in Giambiagi et al., (2003) and Godoy et al., (1999). The cities of Malargüe and San Rafael are given for references. (a) Deformation and erosion of the western Principal Cordilleraand western portion of Malargüe FTB. The synorogenic deposits were accumulated in front or between the growing structures. The previous Late Cretaceous orogenic front would have acted as an eastern barrier for the sediments. The volcanic arc was located in the western Principal Cordillera. (b) Complete development of the Malargüe FTB due to the eastern migration of the deformation. The volcanism also migrated and expended toward the eastern Principal Cordillera. During this period the Frontal Cordillera was uplifted. (c) Maximum eastern expansion of the deformation and volcanism. . The deformation was located around of the Malargüe and San Rafael cities area along with the axial region of the Cordillera. This stage correspond to the main uplift episode of both western Principal Cordillera and San Rafael block. The arc volcanic was around the San Rafael block. (d) Return of the related-arc volcanism to western Principal Cordillera. Moreover, extensional tectonic dominated the foreland along with the eruption of greater basalt flow which built the Payenia Volcanic Field. Toward the west a serie of calderas were formed while the shortening continued in the region.

- Synorogenic deposits evidence that the arc region has underwent shortening since the late Miocene
- Out-of-sequence thrusting event was identified through the southern Central Andes
- Contractional tectonics would dominate the evolution of the arc region since the Pliocene
- The southward increase of the erosion rate would have triggered the out-sequence thrusting in the internal region of the Andes Cordillera

Table 1

Apatite U/Th-He from rocks west of the El Novillo thrust along the valley bottom of the Colorado river

Sample	Unit	Latitude (ºS)	Longitude (ºW)		Corrected apatite U/Th-He Age [Ma] ± 2σ
RC05	Abanico Fm. tuff	35.36	70.62°		1.18 ± 0.71
					0.26 ± 1.21
					1.70 ± 0.41
				Mean weight age	1.47 ±0.12
RC06	Río Negro pluton	35.33	70.68°		3.96 ± 0.13
					3.74 ± 0.10
				Mean weight age	3.83 ± 0.01
RC08	La Gallina pluton	35.31	70.83		3.82 ± 0.12
					3.81 ± 0.70
				Mean weight age	3.82 ± 0.01

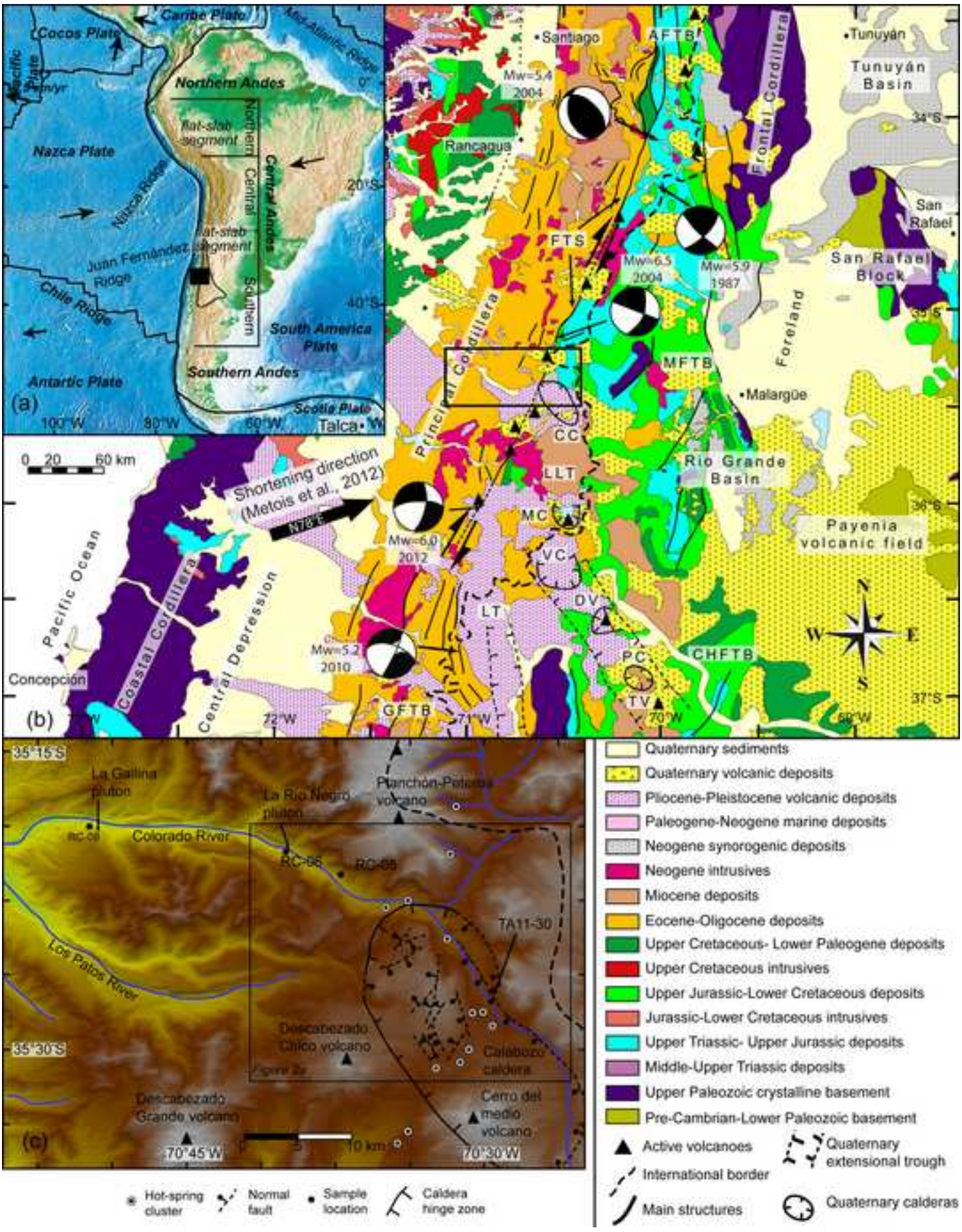

Figure 2

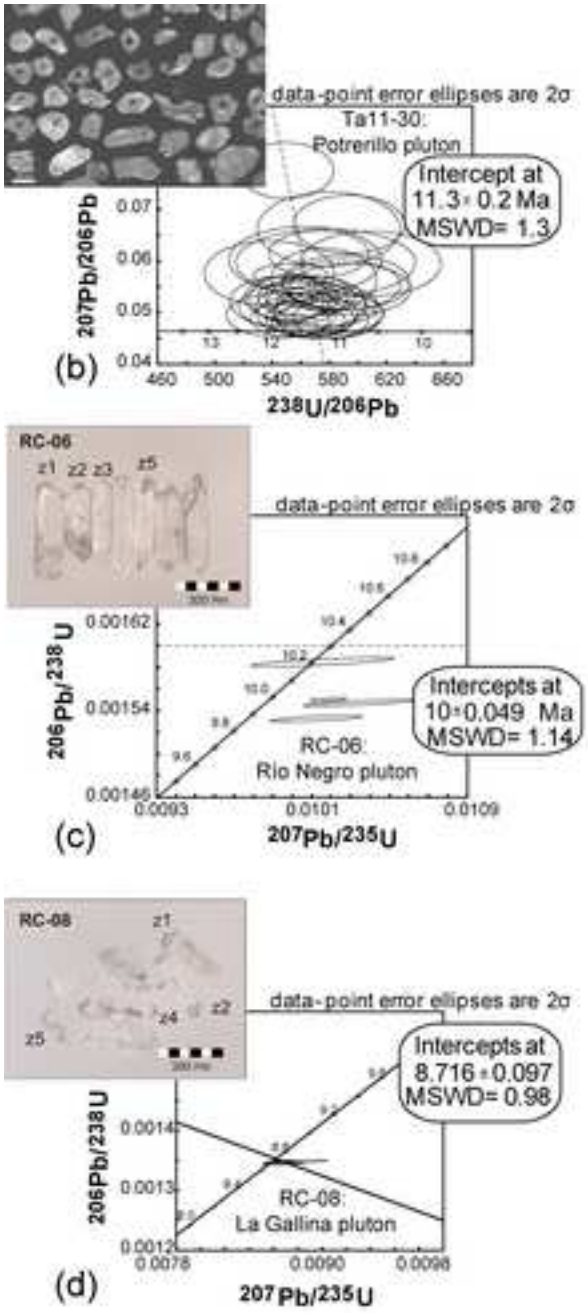
data-point error ellipses are 2σ
Ta11-30:
Potrerillo pluton
Intercept at
11.3 ± 0.2 Ma
MSWD= 1.3
(b)
207Pb/206Pb
238U/206Pb
RC-06
data-point error ellipses are 2σ
Intercepts at
10 ± 0.049 Ma
MSWD= 1.14
RC-06:
Rio Negro pluton
(c)
206Pb/238U
207Pb/235U
RC-08
data-point error ellipses are 2σ
Intercepts at
8.716 ± 0.097
MSWD= 0.98
RC-08:
La Gallina pluton
(d)
206Pb/238U
207Pb/235U

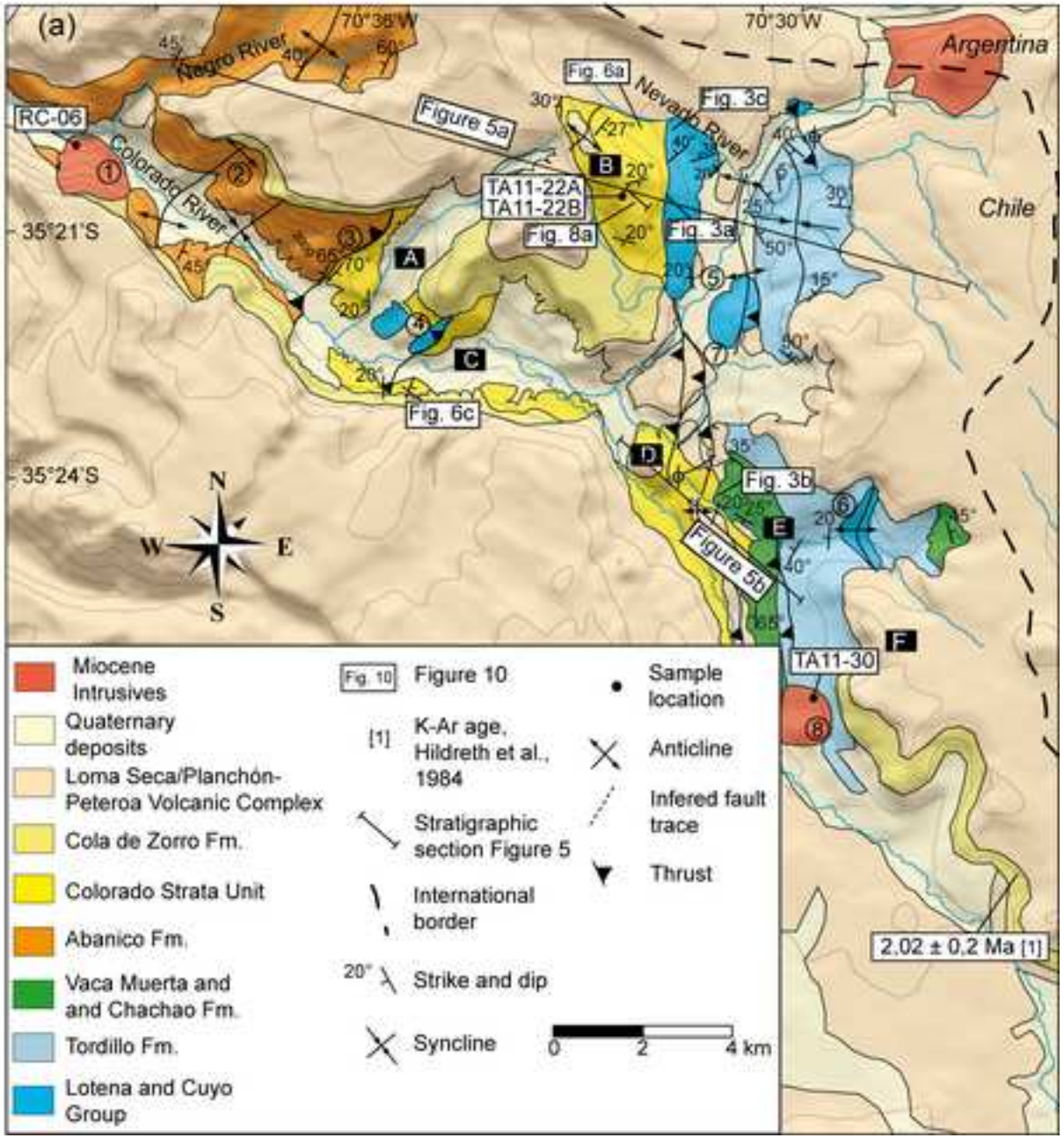
(a)
70°38'W
70°30'W
Argentina
Chile
Negro River
Colorado River
Nevado River
RC-06
Figure 5a
Fig. 6a
Fig. 3c
Fig. 3a
Fig. 8a
TA11-22A
TA11-22B
Fig. 6c
Fig. 3b
Figure 5b
TA11-30
2.02 ± 0.2 Ma [1]
35°21'S
35°24'S
N
W
E
S
A
B
C
D
E
F
Miocene Intrusives
Quaternary deposits
Loma Seca/Planchón-Peteroa Volcanic Complex
Cola de Zorro Fm.
Colorado Strata Unit
Abanico Fm.
Vaca Muerta and and Chachao Fm.
Tordillo Fm.
Lotena and Cuyo Group
Fig. 10 Figure 10
[1] K-Ar age, Hildreth et al., 1984
Stratigraphic section Figure 5
International border
Strike and dip
Syncline
Sample location
Anticline
Infered fault trace
Thrust
0 2 4 km

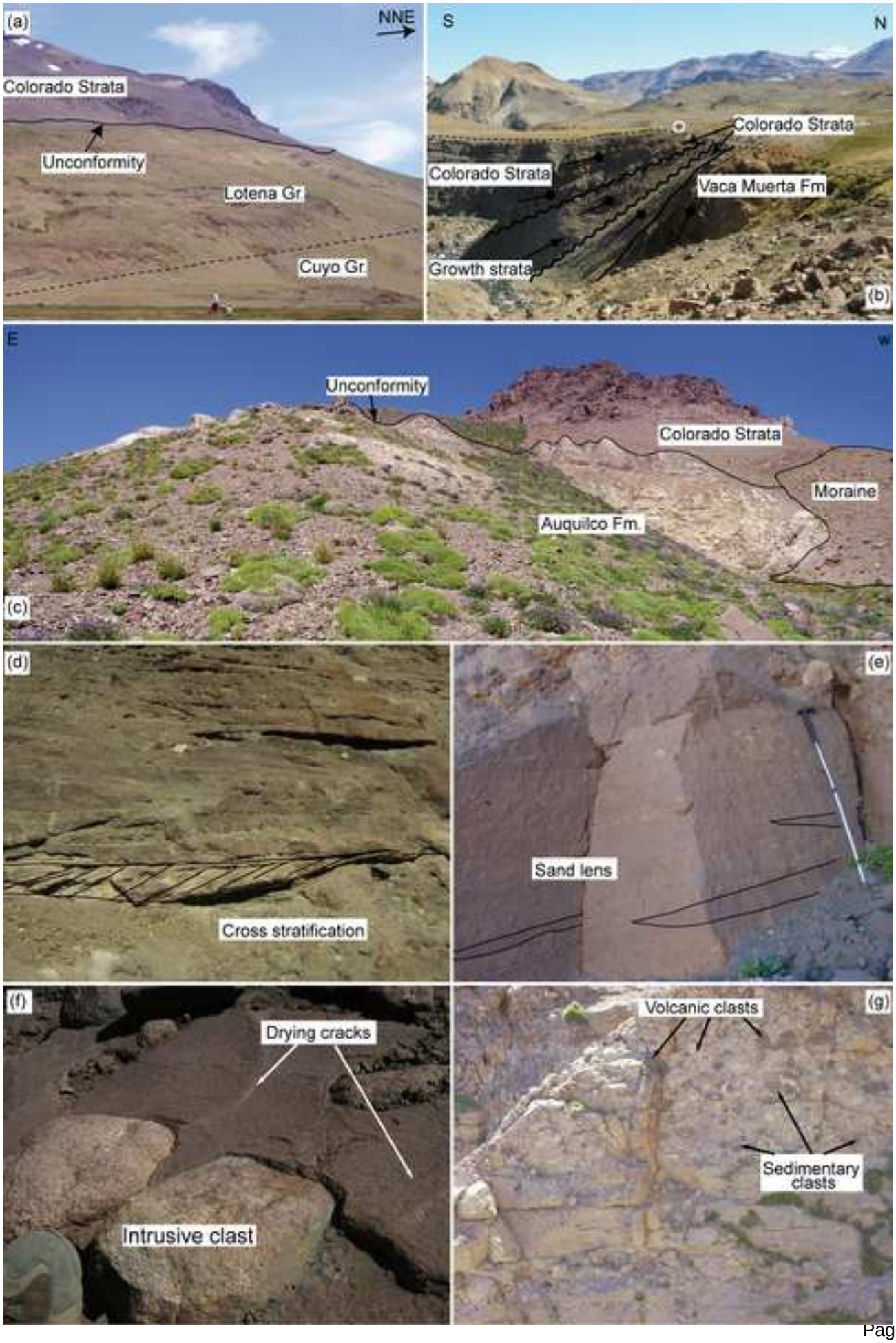

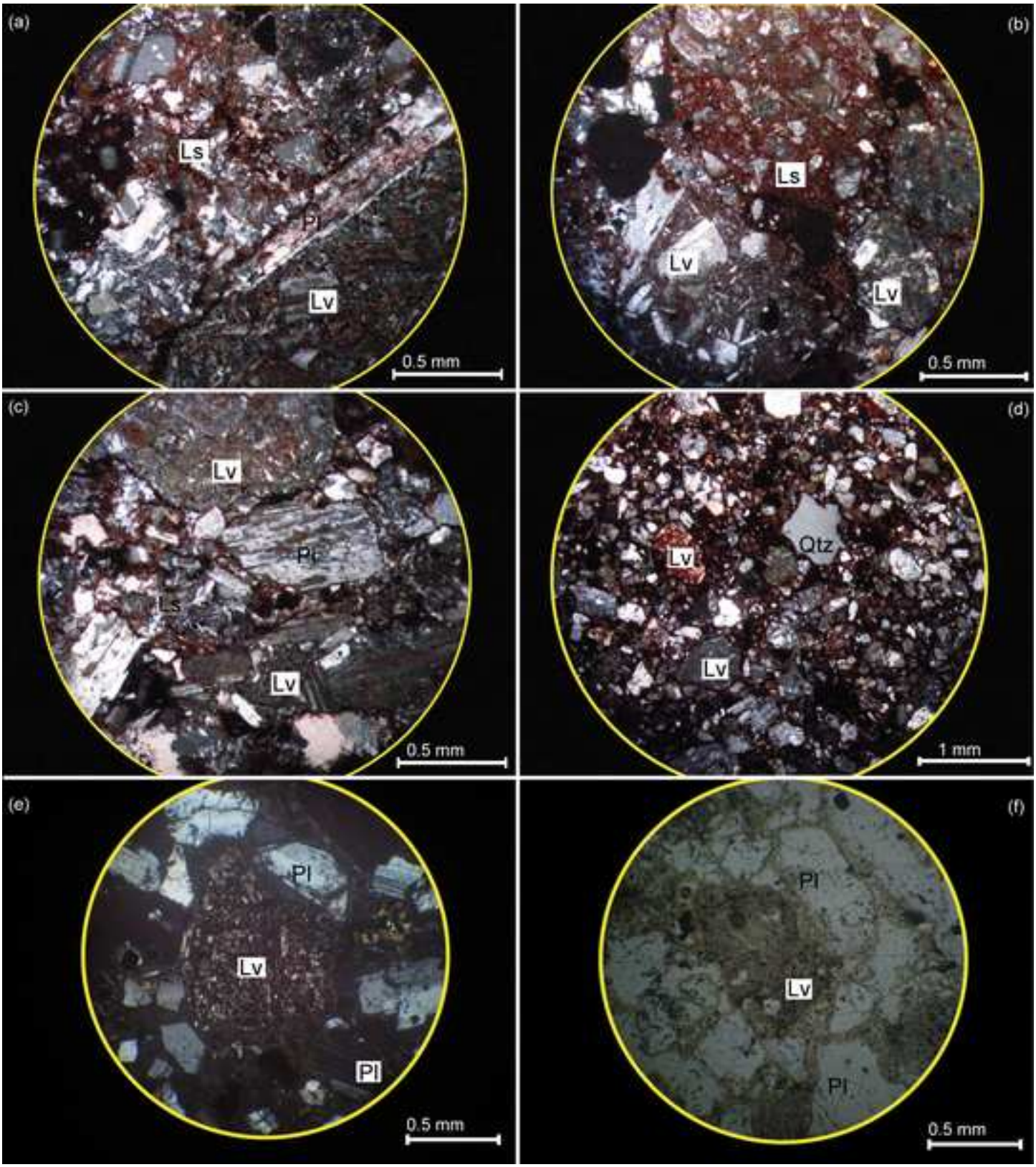

Figure 5

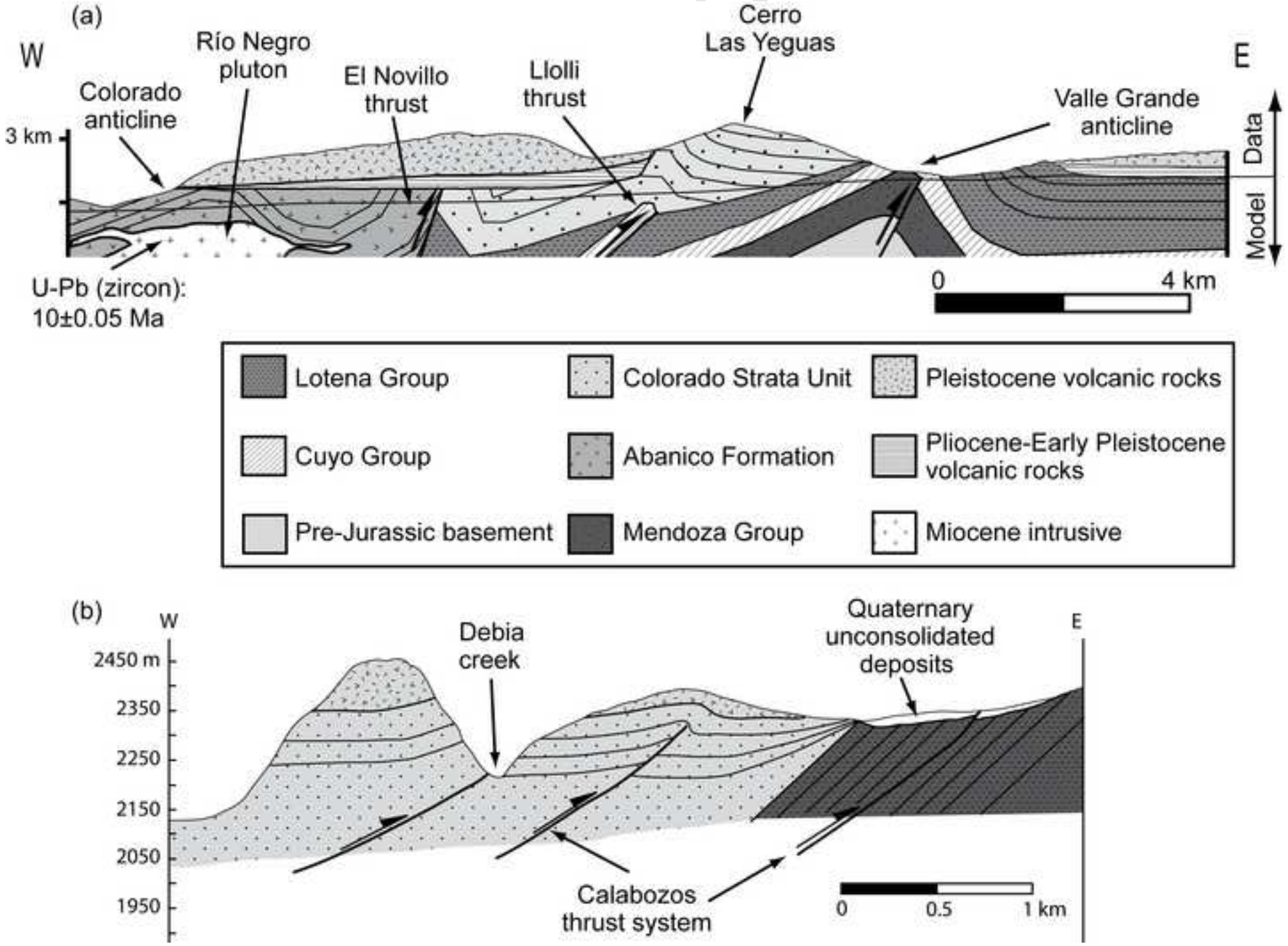
(a)
W
E
Río Negro pluton
El Novillo thrust
Llolli thrust
Cerro Las Yeguas
Colorado anticline
Valle Grande anticline
3 km
Data
Model
U-Pb (zircon): 10±0.05 Ma
0
4 km
Lotena Group
Colorado Strata Unit
Pleistocene volcanic rocks
Cuyo Group
Abanico Formation
Pliocene-Early Pleistocene volcanic rocks
Pre-Jurassic basement
Mendoza Group
Miocene intrusive
(b)
W
E
Debia creek
Quaternary unconsolidated deposits
2450 m
2350
2250
2150
2050
1950
Calabozos thrust system
0
0.5
1 km

Figure 6

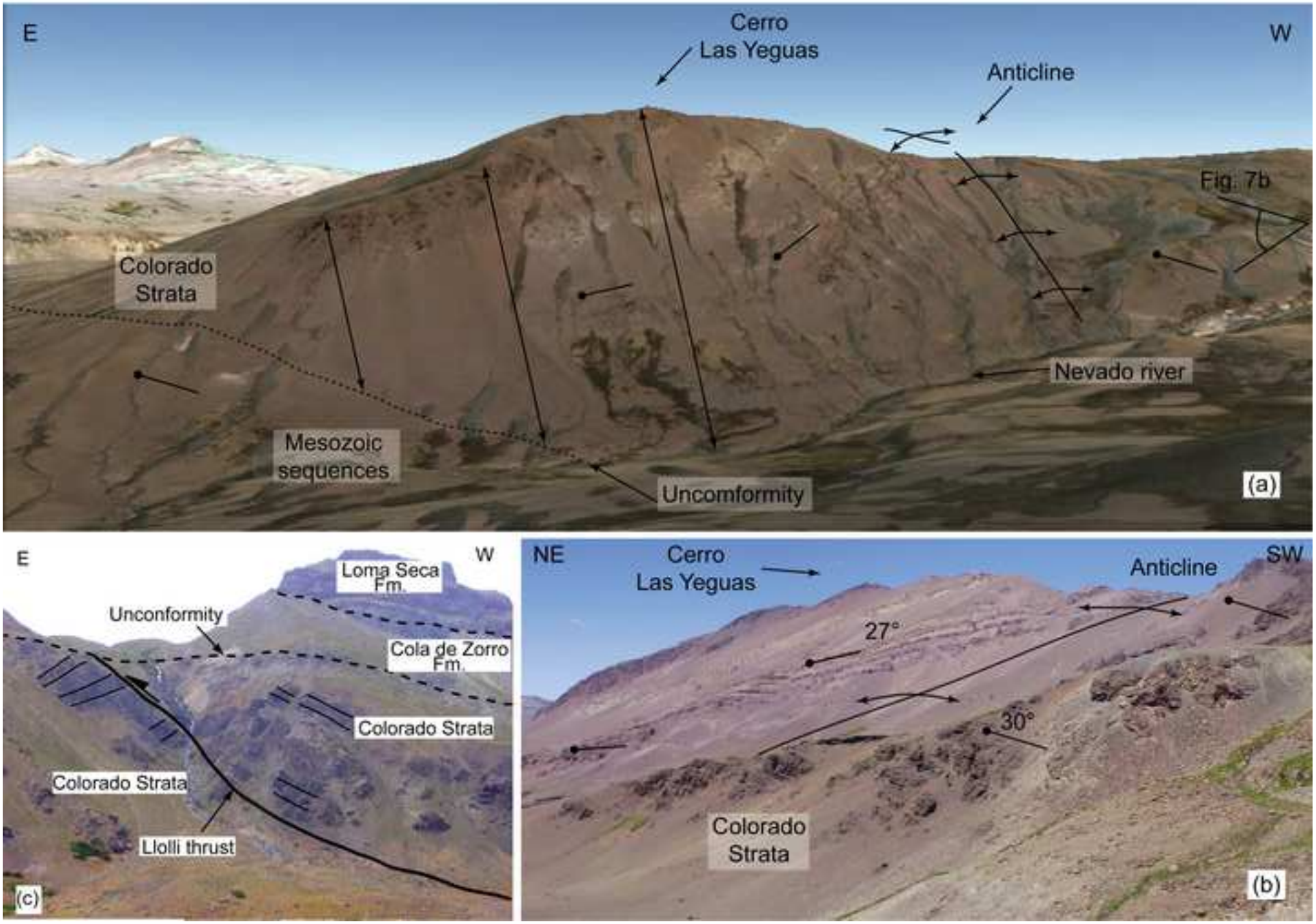
E
W
Cerro
Las Yeguas
Anticline
Fig. 7b
Colorado
Strata
Nevado river
Mesozoic
sequences
Uncomformity
(a)
E
W
Loma Seca
Fm.
Unconformity
Cola de Zorro
Fm.
Colorado Strata
Colorado Strata
Llolli thrust
(c)
NE
SW
Cerro
Las Yeguas
Anticline
27°
30°
Colorado
Strata
(b)

Figure 7

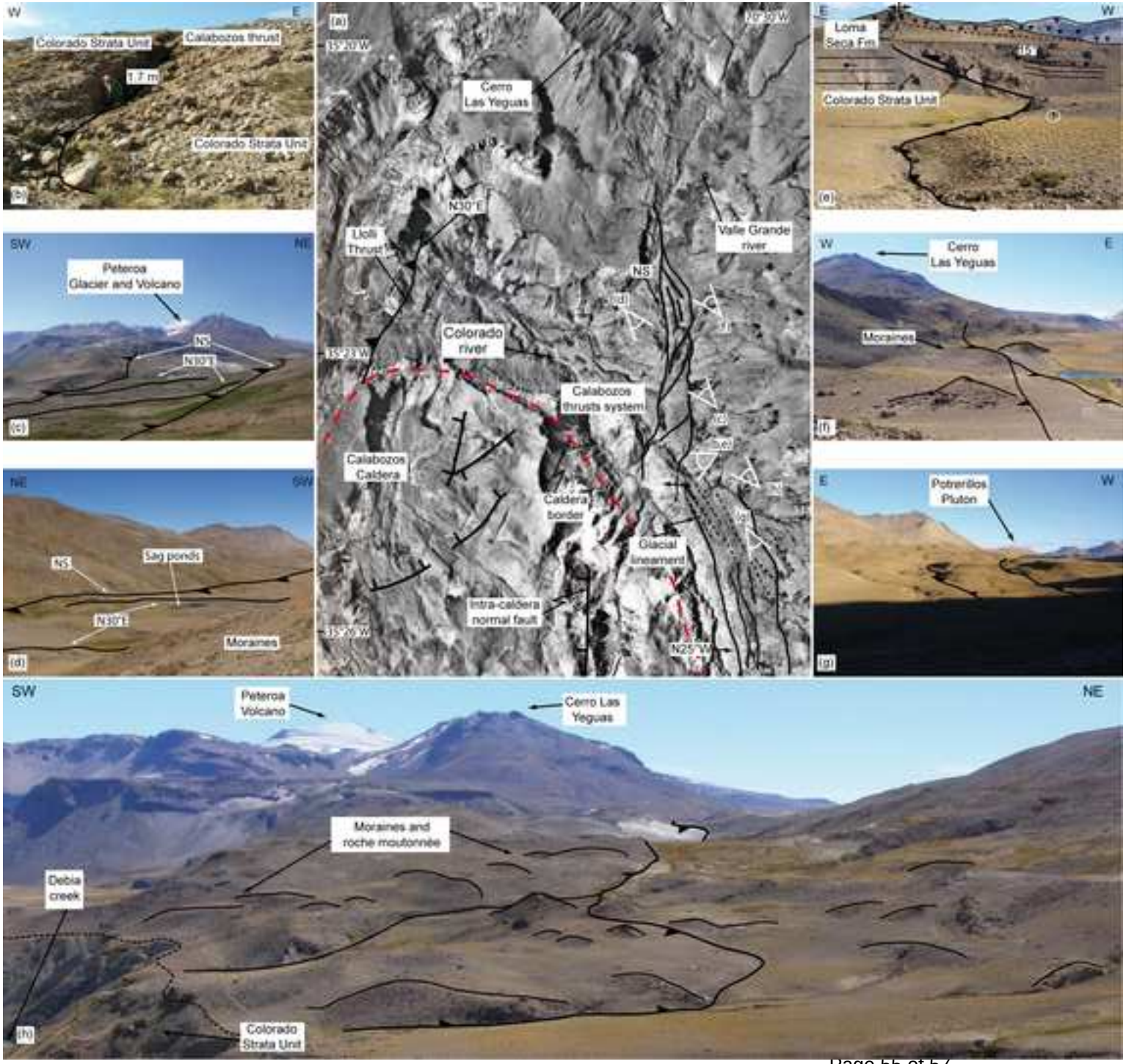
W
E
Colorado Strata Unit
Calabozos thrust
1.7 m
Colorado Strata Unit
(b)
(a)
35°20'W
N70°W
Cerro
Las Yeguas
N30°E
Lloli
Thrust
Valle Grande
river
N-S
Colorado
river
35°23'W
Calabozos
thrusts system
Calabozos
Caldera
Caldera
border
Glacial
lineament
Intra-caldera
normal fault
35°26'W
N25°W
E
W
Loma
Seca Fm
Colorado Strata Unit
(e)
SW
NE
Peteroa
Glacier and Volcano
N-S
N30°E
(c)
W
E
Cerro
Las Yeguas
Moraines
(f)
NE
SW
N-S
Sag ponds
N30°E
Moraines
(d)
E
W
Potrerillos
Pluton
(g)
SW
NE
Peteroa
Volcano
Cerro Las
Yeguas
Moraines and
roche moutonnée
Debia
creek
(h)
Colorado
Strata Unit

Figure 8

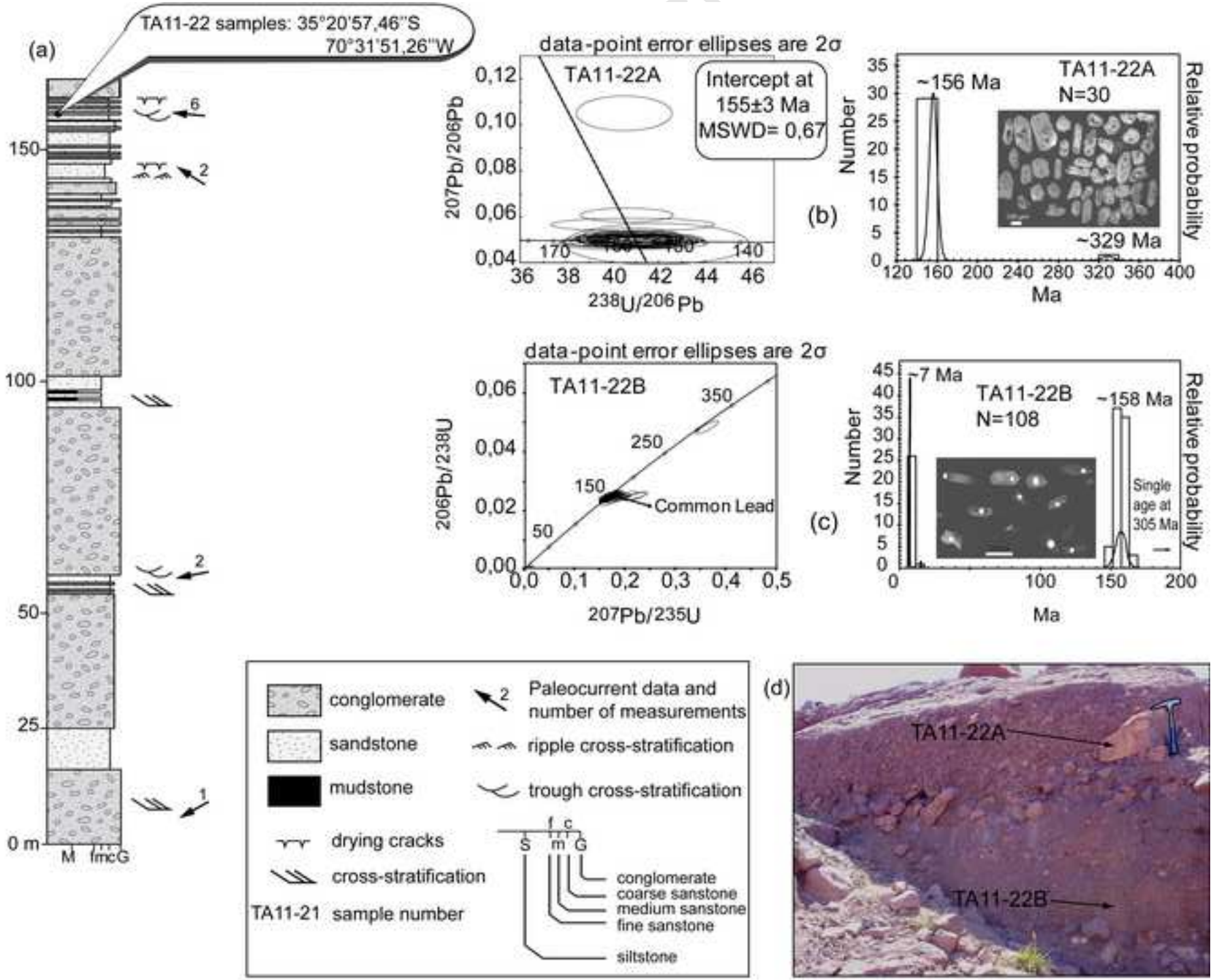
(a)
TA11-22 samples: 35°20'57,46"S
70°31'51,26"W
150
100
50
25
0 m
M fmcG
6
2
2
1
(b)
data-point error ellipses are 2σ
TA11-22A
Intercept at
155±3 Ma
MSWD= 0,67
207Pb/206Pb
238U/206Pb
(c)
data-point error ellipses are 2σ
TA11-22B
Common Lead
206Pb/238U
207Pb/235U
(d)
TA11-22A
~156 Ma
N=30
~329 Ma
Number
Relative probability
Ma
TA11-22B
~7 Ma
~158 Ma
N=108
Single age at 305 Ma
conglomerate
sandstone
mudstone
drying cracks
cross-stratification
TA11-21 sample number
Paleocurrent data and number of measurements
ripple cross-stratification
trough cross-stratification
conglomerate
coarse sanstone
medium sanstone
fine sanstone
siltstone